https://doi.org/10.5194/egusphere-2026-2484
Preprint. Discussion started: 20 May 2026

Technical note: Evaluation of snow water equivalent from large-scale land-surface products over Italy

Gökhan Sarigil[1], Mattia Neri[1], Francesco Avanzi[2], and Elena Toth[1]

[1]Department of Civil, Chemical, Environmental, and Materials Engineering, University of Bologna, Bologna, Italy
[2]CIMA Research Foundation, University Campus of Savona, Savona, Italy

Correspondence to: Mattia Neri (mattia.neri5@unibo.it)

Abstract. Snow water equivalent (SWE) is a critical hydrological variable for water resource management in mountainous regions, where seasonal snowpacks function as natural reservoirs regulating streamflow and water supply. While high-resolution, observation-constrained regional or national snow products provide reliable daily SWE estimates at fine spatial resolution (less than 1 km), their limited temporal coverage often restricts their use for long-term hydro-climatological studies. Large-scale land-surface products, in which SWE is derived from land-surface model simulations driven by atmospheric reanalyses or regional dynamical downscaling systems, provide multi-decadal coverage, but their reliability may be affected by biases in meteorological forcing, limited topographic representation, and simplified snow process parameterisation, requiring rigorous regional evaluation. This study evaluates the SWE estimates of three large-scale land-surface products, i.e., the global ERA5-Land, the European CERRA-Land, and the Italian VHR-REA_IT, against the national reference dataset IT-SNOW across Italy. The analysis combines grid-scale bias assessment of mean annual SWE and snow cover duration with temporal correlation analysis of daily SWE series, and is complemented by an evaluation of precipitation and temperature biases in each product, providing insight into how each product represents the atmospheric conditions governing snow accumulation and ablation and thereby supporting the interpretation of the identified SWE discrepancies. The results show clear regional differences in product performance, with no single product performing best across all metrics. ERA5-Land shows the strongest temporal correlation with IT-SNOW, but tends to overestimate mean annual SWE and snow cover duration in the Alps. CERRA-Land shows more moderate biases than ERA5-Land in the Italian Alps, but generally underestimates mean annual SWE across most subregions, where autumn and winter precipitation deficits in the forcing limit snow accumulation. Across the Apennines, both ERA5-Land and CERRA-Land tend to underestimate SWE and snow cover duration, particularly in the northern sectors. VHR-REA_IT shows widespread underestimation and the weakest temporal correspondence with IT-SNOW: this may be due to its fully coupled atmosphere–land architecture with no assimilation of meteorological observations. Overall, the results suggest that forcing biases explain a substantial part of the observed SWE discrepancies, although not all of them. This study provides useful insights for the use of SWE estimates from large-scale land-surface products in long-term hydro-climatological assessments over Italy and helps to understand whether the products can be used to evaluate snow dynamics in mountainous regions lacking high-quality benchmark estimates.

https://doi.org/10.5194/egusphere-2026-2484
Preprint. Discussion started: 20 May 2026

1 Introduction

Mountain snowpacks function as natural reservoirs, accumulating precipitation during colder months and gradually releasing it as meltwater during warmer seasons. This seasonal regulation sustains streamflow and water availability in snow-dependent regions, supporting ecosystems, agriculture, hydropower, and domestic water supply (e.g. Barnett et al., 2005; Immerzeel et al., 2020; Jenicek et al. 2016). As such, understanding the spatial and temporal distribution of snow is essential for water resource monitoring, streamflow forecasting, flood prediction, and climate change diagnostics (e.g. Bormann et al., 2018; Viviroli et al., 2007).

Snow water equivalent (SWE), defined as the depth of water stored in the snowpack, represents the most direct link to mountain hydrology (King et al., 2020; Takala et al., 2011). However, obtaining reliable and spatially distributed estimates of SWE remains a persistent challenge. Ground-based approaches, including manual snow courses, snow pillows, passive gamma radiation sensors, and cosmic ray neutron sensors, provide valuable site-scale SWE observations through either direct weighing-based measurements or indirect physical inference. But their spatial coverage remains limited due to difficult terrain, adverse weather, and the prohibitive cost of establishing dense observation networks in mountain environments (Bales et al., 2006). These challenges are compounded by the highly variable spatial distribution of snow in mountainous terrain, where SWE can vary dramatically over short distances due to differences in elevation, slope, aspect, and wind exposure (Pflug et al., 2025; Pimentel et al., 2017; Sabetghadam et al., 2025). To overcome these limitations, several approaches have been developed to estimate SWE over large domains.

Satellite remote sensing substantially extends observational coverage beyond ground-based measurements, but current sensor classes still face important limitations for SWE estimation across diverse snow and landscape conditions. Optical sensors, such as MODIS snow cover products (Hall et al., 2002), are effective for mapping snow-covered area, yet they do not provide information on snow depth or SWE. Passive microwave sensors, including AMSR-E and AMSR2, can estimate SWE directly (Kelly, 2009), but their performance is constrained by coarse spatial resolution, signal saturation in deep snowpacks (Chang et al., 1987), and attenuation from forest canopy (Dong et al., 2005). Active microwave products, such as the Sentinel-1-derived C-SNOW dataset (Lievens et al., 2019), offer finer spatial resolution than passive sensors but retrieve snow depth rather than SWE and are mainly applicable under dry-snow conditions, because liquid water in the snowpack absorbs much of the radar signal (Mätzler, 1987; Mirza et al., 2025).

The combined limitations of ground-based measurements and satellite retrievals make it difficult to obtain spatially continuous and temporally consistent SWE estimates across large mountain domains. This challenge has motivated the development of gridded SWE products based on numerical modelling, with varying degrees of snow observation assimilation. High-resolution observation-constrained snow products, typically at ≤1 km resolution, are generated by integrating process-based snow modelling with the assimilation of ground-based and satellite snow observations to produce gridded SWE fields (e.g. Sourp et al., 2026). Prominent examples include IT-SNOW for Italy (~500 m; Avanzi et al., 2023), the Swiss OSHD system (up to ~250 m; Mott et al., 2023), SNODAS for the contiguous United States (~1 km; NOHRSC, 2004), and J-snow for the Po River

https://doi.org/10.5194/egusphere-2026-2484
Preprint. Discussion started: 20 May 2026

District (~500 m; Dall'Amico et al., 2025). Despite their demonstrated reliability, these products are often limited in temporal coverage (e.g., IT-SNOW begins in 2010; SNODAS in 2003), geographical extent (e.g., J-snow covers only the Po River District), or both, because their generation depends on observation systems and supporting datasets that are not always available over long periods or broad domains. This limits their applicability for multi-decadal or large-scale studies.

Large-scale land-surface products, derived from atmospheric reanalyses and regional dynamical downscaling systems that provide continuous meteorological fields over multi-decadal periods, partially overcome the spatial and temporal limitations of observation-constrained snow products by providing internally consistent, gap-free spatiotemporal fields over broad domains. In these systems, SWE is simulated primarily by the snow scheme embedded within the land-surface model, driven by meteorological forcing and, in many cases, without direct assimilation of snow observations. The accuracy of the simulated snowpack is therefore strongly influenced by the quality of the meteorological forcing, which has been identified as a major source of error in snow simulations (Raleigh et al., 2015; Terzago et al., 2020), although its relative importance depends on the modelling framework and application (von Kaenel and Margulis, 2025). Beyond forcing quality, the structure of the snow scheme and the parameterisation of individual snow processes, such as albedo evolution, compaction, and liquid water retention, introduce an additional source of uncertainty (Cho et al., 2022; Günther et al., 2020). This highlights that rigorous validation is required before any land-surface product can be confidently applied for operational purposes.

Although previous studies have evaluated large-scale SWE products in other regions and confirmed that product performance varies with geographic and hydroclimatic setting (Brown et al., 2018; Broxton et al., 2016; Monteiro and Morin, 2023; Mudryk et al., 2025), no systematic evaluation of SWE estimates from large-scale land-surface products has yet been conducted across the whole of Italy. This gap is particularly relevant because the Italian Alps and Apennines are critical headwater regions for national water supply and have experienced marked recent declines in snowpack (Avanzi et al., 2024; Bocchiola and Diolaiuti, 2010), with direct implications for seasonal water availability in downstream basins (Montanari et al., 2023). This study addresses that gap by evaluating SWE estimates from three large-scale land-surface products against IT-SNOW (Avanzi et al., 2023), a high-resolution observation-constrained snow product assimilating dense in situ and satellite snow observations and currently the most reliable gridded SWE reference available for Italy since 2010. The core goal of the evaluation is to assess the potential and limitations of these large-scale products and their underlying land-surface models and atmospheric forcing over the major mountain chains within Italy. The practical implications are twofold: on the national scale, given the limited temporal coverage of IT-SNOW, the results provide guidance for selecting the most suitable product for extending SWE records to prior decades and supporting long-term hydro-climatological assessments; on the continental and global scales, the findings may help characterise the reliability of these products in other hydrologically similar regions that lack high-quality benchmark estimates.

The Technical Note is structured as follows. Section 2 describes the study area. Section 3 presents the reference dataset, IT-SNOW, and the three evaluated products, including their atmospheric forcing and land-surface models. Section 4 describes

https://doi.org/10.5194/egusphere-2026-2484
Preprint. Discussion started: 20 May 2026

the evaluation methodology. Section 5 presents and discusses the evaluation results in terms of mean annual SWE, snow cover duration, and temporal correlation of daily SWE. Section 6 summarises the main findings and their implications.

2 Study area

The study area is Italy, characterised by sharp elevation contrasts where mountain ranges and coastlines combine to shape a great variety of hydrology and climate characteristics (Fig. 1). Elevation varies strongly across the country, from sea level along the extensive Mediterranean coastline to above 4000 m a.s.l. across the highest mountain crests. Italian topography is dominated by two major mountain systems: the Alps, which arc along the northern border and represent the main area of seasonal snow storage and meltwater generation for northern Italy, and the Apennine chain, which forms the backbone of the peninsula and extends for about 1350 km to the Strait of Messina, continuing into northern Sicily. The lower elevation of the Apennines, together with their stronger Mediterranean influence, results in snow cover that is generally less persistent than in the Alps. Marked relief also occurs on the major islands, Sardinia and Sicily.

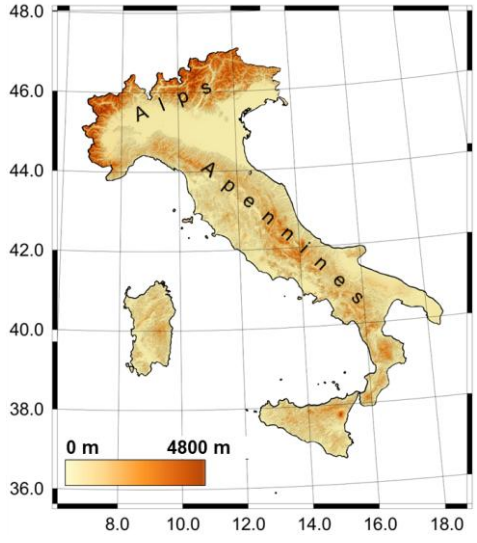

Figure 1. Topographic map of the study domain showing elevation (m a.s.l.) across Italy.

The topographic contrasts described above translate into marked spatial gradients in climatic conditions and snow storage across Italy. Figure 2 summarises this variability through mean annual precipitation (panel a), mean annual temperature (panel b), and mean annual SWE (panel c), all computed as temporal averages of daily values over the study period from September 2010 to August 2024. The precipitation and temperature fields are derived from SCIA (Desiato et al., 2007, 2011), a national gridded observational dataset, whereas SWE is derived from IT-SNOW (Avanzi et al., 2023), the high-resolution observation-constrained snow product for Italy that is here used as the reference SWE product. These datasets are used here to characterise

https://doi.org/10.5194/egusphere-2026-2484
Preprint. Discussion started: 20 May 2026

the study area, while their full description and role in the evaluation are provided later in Sect. 3.1 for IT-SNOW and Sect. 4.2 for SCIA.

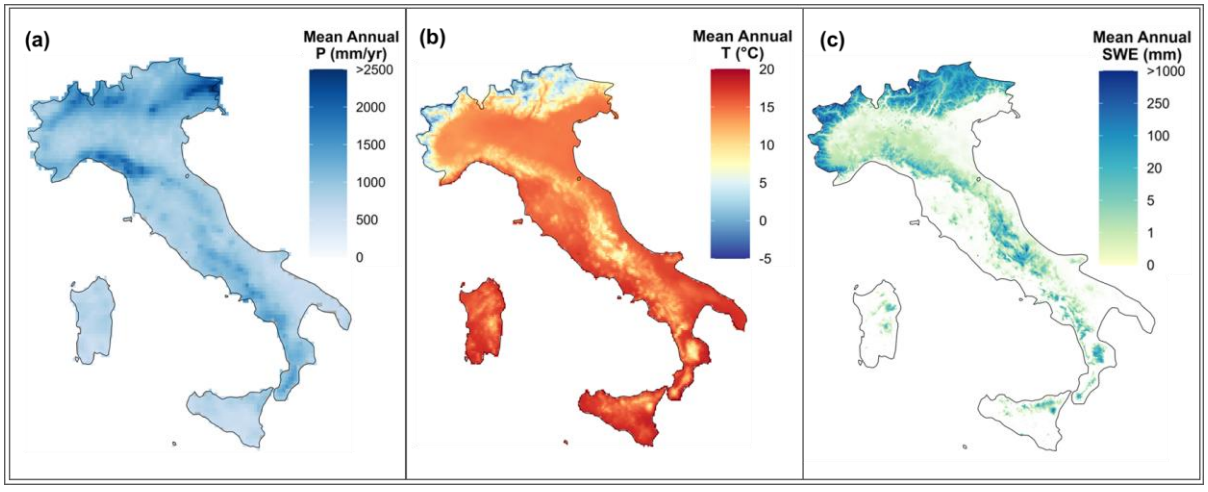

Figure 2. Climatic and snow regime characteristics of the study area for the period 2010 to 2024: (a) mean annual precipitation and (b) mean annual temperature from the SCIA observational dataset, and (c) mean annual snow water equivalent from the IT-SNOW reference dataset.

Figure 2 highlights the marked spatial variability of climate and snow conditions across Italy. Mean annual precipitation (panel a) reflects the influence of orography (Frei and Schär, 1998), with the highest values along the Alpine arc and the northern Apennines, particularly in the Ligurian sector, where moisture from the Mediterranean is enhanced by uplift (Miglietta and Davolio, 2022), while lower values occur across lowland areas and the major islands. Mean annual temperature (panel b) follows the main elevation gradient, with the coldest conditions in the highest Alpine sectors, intermediate values along the Apennine ridge, and the warmest conditions in coastal areas, plains, and the islands. Together, these precipitation and temperature patterns shape the spatial distribution of mean annual SWE (panel c). The highest SWE values occur in the Alps, where high elevations maintain colder conditions, increase the fraction of precipitation falling as snow, and delay melt. In the Apennines, SWE is generally lower and more spatially heterogeneous, despite moderate precipitation in several sectors, because milder conditions limit snow accumulation and persistence. In the plains and coastal areas, mean annual SWE is close to zero. Overall, these contrasts, from the larger and more persistent Alpine snowpacks to the smaller and more intermittent Apennine snow cover, make Italy well suited for evaluating land-surface products across a wide range of snow regimes.

https://doi.org/10.5194/egusphere-2026-2484
Preprint. Discussion started: 20 May 2026

3 Datasets and product descriptions

3.1 Reference SWE dataset: IT-SNOW

IT-SNOW is a high-resolution, observation-constrained snow reanalysis for Italy, providing daily maps of SWE, snow depth, bulk snow density, and liquid water content at ~500 m spatial resolution (Avanzi et al., 2023). The product is heavily constrained by extensive in situ and satellite snow data through assimilation within the S3M (Snow Multidata Mapping and Modeling) distributed cryospheric model (Avanzi et al., 2022), developed by CIMA Research Foundation for the Italian Civil Protection Department.

Meteorological forcing is derived from a very dense network of automatic weather stations providing hourly precipitation, air temperature, relative humidity, and incoming shortwave radiation. Precipitation fields (~1 km resolution) are generated using a modified conditional merging approach that blends rain gauge observations with radar data through the GRISO algorithm (Bruno et al., 2021). Air temperature is spatialised through region-specific hourly linear regressions against elevation, fitted within meteorological homogeneous regions defined by the Italian Civil Protection. Relative humidity and incoming shortwave radiation are spatialised using inverse distance weighting. Precipitation phase partitioning is determined within the model using air temperature and relative humidity (Froidurot et al., 2014).

S3M solves the snow mass balance using a single-layer scheme with hybrid temperature-index and radiation-driven melt, snow settling, liquid water outflow, and albedo evolution (Avanzi et al., 2022). Glacier areas, identified from the Randolph Glacier Inventory v6.0 (Pfeffer et al., 2014), are handled separately within the model, so that the IT-SNOW SWE fields represent only seasonal snowpack. IT-SNOW assimilates snow observations daily using two complementary data sources. The first is a blended snow-covered area map combining Sentinel-2 (Main-Knorn et al., 2017), MODIS, and EUMETSAT H SAF products. The second is a set of snow depth maps obtained by interpolating observations from ~350 ultrasonic sensors across Italy: within each of 10 homogeneous snow regions, daily multilinear regressions against elevation, slope, and aspect are used to spatialise point observations into gridded snow depth fields, which are then converted to SWE using modelled snow density and used to correct the modelled snowpack with spatially varying weights based on sensor proximity.

IT-SNOW has been evaluated against Sentinel-1-derived snow depth maps (C-SNOW; Lievens et al., 2019) and independent in situ snow depth and SWE measurements (Avanzi et al., 2023). Snow depth estimates have been shown to be consistent with satellite-based snow data, with low mean bias across the Italian landscape, and comparison against ground measurements confirms that the dataset reconstructs seasonal snow accumulation and melt dynamics.

3.2 Evaluated large-scale land-surface products

The products evaluated in this study differ in both product architecture and the way observational information enters the modelling system. Because these structural differences directly affect how biases originate and propagate into the simulated

https://doi.org/10.5194/egusphere-2026-2484
Preprint. Discussion started: 20 May 2026

SWE fields, understanding them provides the basis for interpreting the evaluation results. This requires distinguishing the role of the atmospheric component from that of the land-surface modelling component in each product.

Atmospheric reanalyses reconstruct past atmospheric conditions by reprocessing the historical observing record with a fixed numerical weather prediction model and data assimilation system (Baatz et al., 2021). The atmospheric model solves the governing equations for mass, momentum, and energy, advancing prognostic state variables such as air temperature, humidity, wind components, and surface pressure, which together describe the instantaneous state of the atmosphere. Data assimilation updates this model state, adjusting the prognostic variables to bring the analysed atmospheric state into closer agreement with available observations while maintaining consistency with the model dynamics (Kalnay, 2003). In conventional atmospheric reanalyses, precipitation and the turbulent fluxes of latent and sensible heat differ in nature from the prognostic state variables: they do not describe the atmosphere at an instant but represent transfers of mass and energy over a time interval, and are typically diagnosed from the evolving model state rather than analysed directly. They are generated by the model itself, with precipitation produced within the atmospheric column by the cloud microphysics and convection schemes, and the turbulent surface fluxes evaluated at the land–atmosphere interface from the model atmospheric state and the prescribed or simulated surface conditions (Betts et al., 1996).

Simulating SWE and other land-surface variables requires a land-surface model with dedicated schemes for snow, soil, and vegetation processes. Two main configurations are commonly used for running such a model: offline and coupled (Masson et al., 2013). In an offline configuration, the land-surface model is driven by meteorological forcing fields and does not return energy or moisture fluxes to the atmosphere. These forcing fields may come directly from a global atmospheric reanalysis or from a regional atmospheric model or reanalysis that dynamically downscales a larger-scale driving system to higher resolution (Giorgi and Mearns, 1999; Laprise, 2008). In a coupled configuration, the land-surface scheme is integrated within the atmospheric model, and the two components exchange energy, moisture, and momentum continuously (Betts et al., 1996). Such coupling allows land–atmosphere feedbacks to develop, but also permits biases in either component to propagate through the coupled system (Santanello et al., 2018). The main characteristics of the three evaluated products, including their atmospheric forcing source, land-surface model, and coupling configuration, are summarised in Table 1.

https://doi.org/10.5194/egusphere-2026-2484
Preprint. Discussion started: 20 May 2026

Table 1. Main characteristics of the large-scale land-surface products evaluated in this study.

Dataset	Spatial and temporal coverage	Resolution	Atmospheric model	Land-surface model	Produced by
ERA5-Land (Muñoz-Sabater et al., 2021)	Global, 1950–present	~9 km, Hourly	IFS (ERA5 atmospheric forcing)	CHTESSEL	ECMWF / Copernicus C3S
CERRA-Land (Verrelle et al., 2022)	Europe, 1984–present	5.5 km, 3-hourly	HARMONIE-ALADIN (CERRA atmospheric forcing)	SURFEX	ECMWF / Copernicus C3S
VHR-REA_IT (Raffa et al., 2021)	Italy, 1981–present	~2.2 km, Hourly	COSMO-CLM	TERRA-ML	CMCC

The fifth-generation ECMWF reanalysis ERA5 is the common upstream global reanalysis from which all three evaluated products derive their atmospheric information, though in different ways. ERA5 is produced within the Copernicus Climate Change Service based on the Integrated Forecasting System at approximately 31 km horizontal resolution (Hersbach et al., 2020). Its atmospheric state is constrained through a hybrid incremental four-dimensional variational data assimilation system (Courtier et al., 1994), in which observations are assimilated within 12-hour windows using short-range forecasts as the background. The assimilated observing system includes surface stations, radiosondes, aircraft, ships, buoys, and a large volume of satellite radiances (Soci et al., 2024).

The differences in how each of the analysed products uses this common source are relevant for interpreting their SWE estimates: ERA5-Land is driven directly by ERA5 atmospheric forcing fields, CERRA-Land receives its forcing through the intermediate regional atmospheric reanalysis CERRA (Ridal et al., 2024), for which ERA5 provides lateral boundary conditions, and VHR-REA_IT uses ERA5 only as lateral boundary conditions within a fully coupled regional atmosphere–land system. The following subsections describe each product in more detail, focusing on the atmospheric forcing chain and the snow scheme.

3.2.1 ERA5-Land

ERA5-Land is a global land-surface reanalysis produced by the European Centre for Medium-Range Weather Forecasts (ECMWF), providing land variables at approximately 9 km (0.1°) resolution from 1950 to near-present (Muñoz-Sabater et al., 2021). The dataset is generated by running the CHTESSEL land-surface model (Balsamo et al., 2009) in offline mode, driven by atmospheric forcing derived from the ERA5 reanalysis (Hersbach et al., 2020).

To achieve the higher spatial resolution, the forcing fields are spatially downscaled from ERA5's ~31 km grid to ERA5-Land's 9 km resolution. Precipitation is redistributed through linear interpolation from ERA5 to the 9 km grid, without any further

https://doi.org/10.5194/egusphere-2026-2484
Preprint. Discussion started: 20 May 2026

correction, whereas temperature, humidity, and pressure from ERA5's lowest model level (approximately 10 m above the surface) are interpolated and corrected for elevation differences using daily lapse rates. Notably, the 2-meter temperature is not directly downscaled from ERA5 but is computed internally by CHTESSEL from the surface energy balance: the model first solves for the skin temperature (i.e., the radiative temperature of the outermost surface) and then estimates the 2-meter temperature by interpolating between this value and the elevation-corrected 10-meter temperature.

CHTESSEL uses a single-layer bulk snow scheme (Dutra et al., 2010) that represents the entire snowpack as a single homogeneous layer with uniform temperature, density, and liquid water content. In ERA5-Land, liquid and solid precipitation are inherited from the ERA5 forcing and then interpolated to the 9 km ERA5-Land grid, so snowfall provides the solid input to the snow scheme rather than being diagnosed independently within the offline land-surface integration. The snow mass balance includes accumulation from snowfall, melting derived from the surface energy balance, and losses through sublimation. Snow density increases due to compaction and metamorphism, while snow albedo is reset toward its maximum after snowfall and then decays linearly during non-melting conditions and exponentially during melting conditions. The model lacks a dedicated glacier component; grid cells with more than 50 % ice cover are instead assigned a constant snow mass equivalent to 10 m water equivalent throughout the simulation.

ERA5-Land does not assimilate any land-surface observations; the only observational constraint enters the system through the assimilated atmospheric state of ERA5, from which the forcing fields are derived. Consequently, biases in the downscaled forcing fields can propagate into the SWE simulations without any observational correction at the land surface.

3.2.2 CERRA-Land

CERRA-Land provides European regional land-surface reanalysis at 5.5 km resolution and three-hourly frequency, covering September 1984 to present (Verrelle et al., 2022). The dataset is generated by running the SURFEX v8.1 land-surface model (SURFace EXternalisée; Masson et al., 2013) in offline mode, driven by meteorological forcing from the parent CERRA regional atmospheric reanalysis.

The CERRA atmospheric reanalysis (Ridal et al., 2024) is produced by running the HARMONIE-ALADIN regional atmospheric model (Bengtsson et al., 2017) at 5.5 km resolution over Europe, with ERA5 providing the lateral boundary conditions. Within the regional domain, CERRA develops its own atmospheric fields through higher-resolution dynamics and data assimilation, using conventional observations, satellite radiances, atmospheric motion vectors, and GNSS radio occultation data to constrain the atmospheric state. CERRA-Land adds the land-surface component to this atmospheric system at the same 5.5 km resolution. No land-surface observations are assimilated; however, before entering the land-surface model, the precipitation forcing undergoes a gauge-based correction.

Precipitation forcing in CERRA-Land is based on a daily gauge-corrected precipitation analysis produced with MESCAN and temporally disaggregated to 3-hourly resolution. Liquid and solid precipitation inputs are then derived from this corrected precipitation forcing through rain-snow partitioning following Froidurot et al. (2014), using the near-surface atmospheric fields

https://doi.org/10.5194/egusphere-2026-2484
Preprint. Discussion started: 20 May 2026

provided by CERRA. CERRA-Land is therefore the only evaluated product whose forcing chain includes an explicit gauge-based correction of precipitation. Over Italy, however, the effectiveness of this adjustment is limited by the sparse gauge coverage available to MESCAN (Soci et al., 2016), so across much of the domain the precipitation forcing remains strongly dependent on the CERRA atmospheric model output. The 2 m temperature, by contrast, is passed directly from the CERRA atmospheric reanalysis to CERRA-Land without re-computation, since HARMONIE-ALADIN already diagnoses 2 m temperature as a standard output of the atmospheric model. This differs from ERA5-Land, where the 2 m temperature is not taken from ERA5 but is derived internally by CHTESSEL through interpolation between the skin temperature solved from the surface energy balance and the elevation-corrected lowest-level atmospheric temperature.

SURFEX implements snow processes through the ISBA-ES (Interactions between Soil, Biosphere, and Atmosphere, Explicit Snow) multi-layer scheme (Boone and Etchevers, 2001; Vionnet et al., 2012), which divides the snowpack into 12 layers (Decharme et al., 2016). Each layer carries prognostic variables for temperature, density, and liquid water content, with thinner layers near the surface to resolve melt processes. The scheme simulates inter-layer heat transfer, liquid water percolation through a bucket approach and wind-driven densification, and computes the full surface energy balance to determine snowmelt rate (Essery et al., 2013). This multi-layer structure allows the representation of vertical temperature gradients and internal processes that single-layer schemes such as CHTESSEL cannot resolve.

3.2.3 VHR-REA_IT

The Very High-Resolution Reanalysis for Italy (VHR-REA_IT) is a regional dynamical downscaling product for Italy produced by the Centro Euro-Mediterraneo sui Cambiamenti Climatici (CMCC), providing hourly variables at 2.2 km (0.02°) resolution for the period 1981 to near-present (Raffa et al., 2021). Unlike ERA5-Land and CERRA-Land, VHR-REA_IT is not generated through an offline land-surface simulation. Instead, the COSMO-CLM regional atmospheric model (Rockel et al., 2008) and the TERRA-ML land-surface model (Schrodin and Heise, 2001) run as a fully coupled system, exchanging fluxes of energy and moisture at every timestep.

Because VHR-REA_IT is produced with a fully coupled regional atmosphere–land modelling system, near-surface forcing fields are generated internally by the regional model rather than supplied through a separate offline forcing dataset. COSMO-CLM generates its own atmospheric fields at convection-permitting resolution, where deep convection is explicitly resolved while only shallow convection is parameterised (Doms et al., 2024). The atmospheric model is driven at its lateral boundaries by ERA5, with boundary conditions updated every 3 hours; within the domain, the regional atmosphere evolves freely through its own dynamics (Loprieno et al., 2024). No observational data are assimilated within the regional domain, so the only observational constraint on VHR-REA_IT enters indirectly through the ERA5 lateral boundary conditions. The two-way coupling allows land–atmosphere feedbacks to develop, but also permits biases in either component to propagate through the coupled system. The atmospheric model provides the land-surface scheme with separate liquid and solid precipitation components, while their partitioning is determined within the atmospheric model.

https://doi.org/10.5194/egusphere-2026-2484
Preprint. Discussion started: 20 May 2026

Snow processes are handled by TERRA-ML, which represents the land surface through multiple soil layers but treats the snowpack as a single bulk reservoir. Snow accumulation increases the water content of this reservoir, while melt is computed from the coupled surface energy and water balance and contributes liquid water to the soil system. The model also accounts for phase changes between liquid and frozen water at the surface and within the soil (Doms et al., 2024).

4 Evaluation methodology

4.1 Data processing and SWE comparison setup

The comparison covers 14 snow-years from September 2010 to August 2024. The start of this period is determined by the availability of the IT-SNOW reference dataset, while the end date is constrained by the SCIA observational dataset (Desiato et al., 2007, 2011), which is used for the complementary forcing evaluation described in Sect. 4.2 and, at the time of this analysis, is available through the end of 2024. The analysis is restricted to grid cells where IT-SNOW mean annual SWE exceeded 1 mm in at least one year during the study period, so that the evaluation focuses on areas where seasonal snow is relevant.

The SWE estimates were evaluated using three grid-scale indicators, each targeting a different aspect of snowpack representation:

- mean annual SWE, computed by averaging daily SWE over each hydrological year and then across the full study period, quantifies the overall snow mass estimated by each product.
- snow cover duration (SCD), defined as the mean annual number of days with SWE exceeding 5 mm, characterises snowpack persistence; the 5 mm threshold was adopted to distinguish meaningful snow presence from marginal snow amounts, consistent with previous studies using the same threshold for snow-cover identification from SWE fields (Dawson et al., 2018; Di Marco et al., 2021; Jenicek et al., 2021; Matiu and Hanzer, 2022).
- the Pearson correlation coefficient between the daily SWE series of each product and the IT-SNOW reference, calculated at each grid cell over the study period, evaluates the ability of each product to reproduce day-to-day snowpack variability irrespective of magnitude bias.

The four datasets differ substantially in native resolution (IT-SNOW: ~500 m; VHR-REA_IT: 2.2 km; CERRA-Land: 5.5 km; ERA5-Land: ~9 km). Therefore, these indicators cannot be compared directly without spatial harmonisation. To enable a consistent quantitative intercomparison, the datasets were re-gridded to a common spatial framework (Lindsay et al., 2014; Mudryk et al., 2025). For mean annual SWE and SCD, the indicators were first computed at each product's native resolution to preserve spatial gradients in complex terrain and to prevent the distortion of threshold-based statistics by prior spatial averaging (Matiu et al., 2021; Rajulapati et al., 2020). The resulting indicator fields were then re-gridded to the coarsest grid (ERA5-Land, ~9 km) through first-order conservative remapping (Jones, 1999), and pixel-wise bias was obtained by subtracting the IT-SNOW indicator from the corresponding product indicator on this common grid. Mean annual SWE and

https://doi.org/10.5194/egusphere-2026-2484
Preprint. Discussion started: 20 May 2026

SCD are presented at native resolution to preserve the full detail of each product, while their bias maps are shown on the common 9 km grid to allow a consistent quantitative comparison. Daily correlation required a different approach: because the Pearson coefficient must be computed from paired time series at matching grid cells, daily SWE fields were first re-gridded to the common 9 km grid through first-order conservative remapping, and the correlation was then computed pixel-wise over the full study period.

4.2 Complementary evaluation of atmospheric forcing

Precipitation and temperature are the main atmospheric controls on snow accumulation and ablation, and biases in these fields can contribute to discrepancies in simulated SWE (Monteiro and Morin, 2023; Terzago et al., 2020). Evaluating the precipitation and temperature estimates of each of the three products here analysed against an independent observational reference therefore provides useful context for interpreting the corresponding SWE discrepancies, although these discrepancies may also reflect other factors related to model structure and process representation.

The meteorological observational reference used for this purpose is SCIA (Desiato et al., 2007, 2011), maintained by the Italian Institute for Environmental Protection and Research (ISPRA). SCIA provides daily gridded precipitation at 10 km resolution from 1961 onwards and minimum/maximum temperature at 5 km resolution from 1981 onwards, both derived from a high-density network of regional meteorological stations. The dataset has been widely adopted as a reference in Italian hydrological studies (e.g., Moccia et al., 2025; Sarigil et al., 2024), and its availability through the end of 2024 at the time of this analysis defines the end date of the study period adopted in this work.

For each product, mean annual and seasonal biases in precipitation and temperature relative to SCIA were computed at native resolution and re-gridded to the common 9 km grid following the same procedure described in Sect. 4.1. These comparisons were used as a complementary diagnostic to support the interpretation of the SWE evaluation.

Given that a comprehensive standalone assessment of gridded meteorological products over Italy is not the main scope of this study, the forcing comparison is presented in the Appendices rather than in the main text: Appendix A reports the mean annual biases (Fig. A1 for precipitation, Fig. A2 for temperature), and Appendix B reports the seasonal biases in precipitation, temperature, and SWE for each product (Fig. B1 for ERA5-Land, Fig. B2 for CERRA-Land, Fig. B3 for VHR-REA_IT). These figures are referenced throughout Sect. 5 to support the interpretation of the SWE evaluation results.

5 Results and discussion

5.1 Mean annual SWE

The initial phase of the assessment is the comparison of the mean annual SWE estimates from each product. The results are presented in Fig. 3: figure's top row (panels a–d) displays the mean annual SWE from the IT-SNOW reference and the three land-surface products at their native resolution, allowing for a direct visualisation of their respective spatial distributions and

https://doi.org/10.5194/egusphere-2026-2484
Preprint. Discussion started: 20 May 2026

magnitudes; in addition, to quantify the discrepancies from the reference data, the second row (panels e–g) presents bias maps calculated as the difference between each of the three land-surface products and the reference (Product − IT-SNOW), so that negative (red colour) values represent where the product underestimates the reference values and positive (blue colour) values represent an overestimation. For this comparison, the datasets resampled to the ERA5-Land resolution are used.

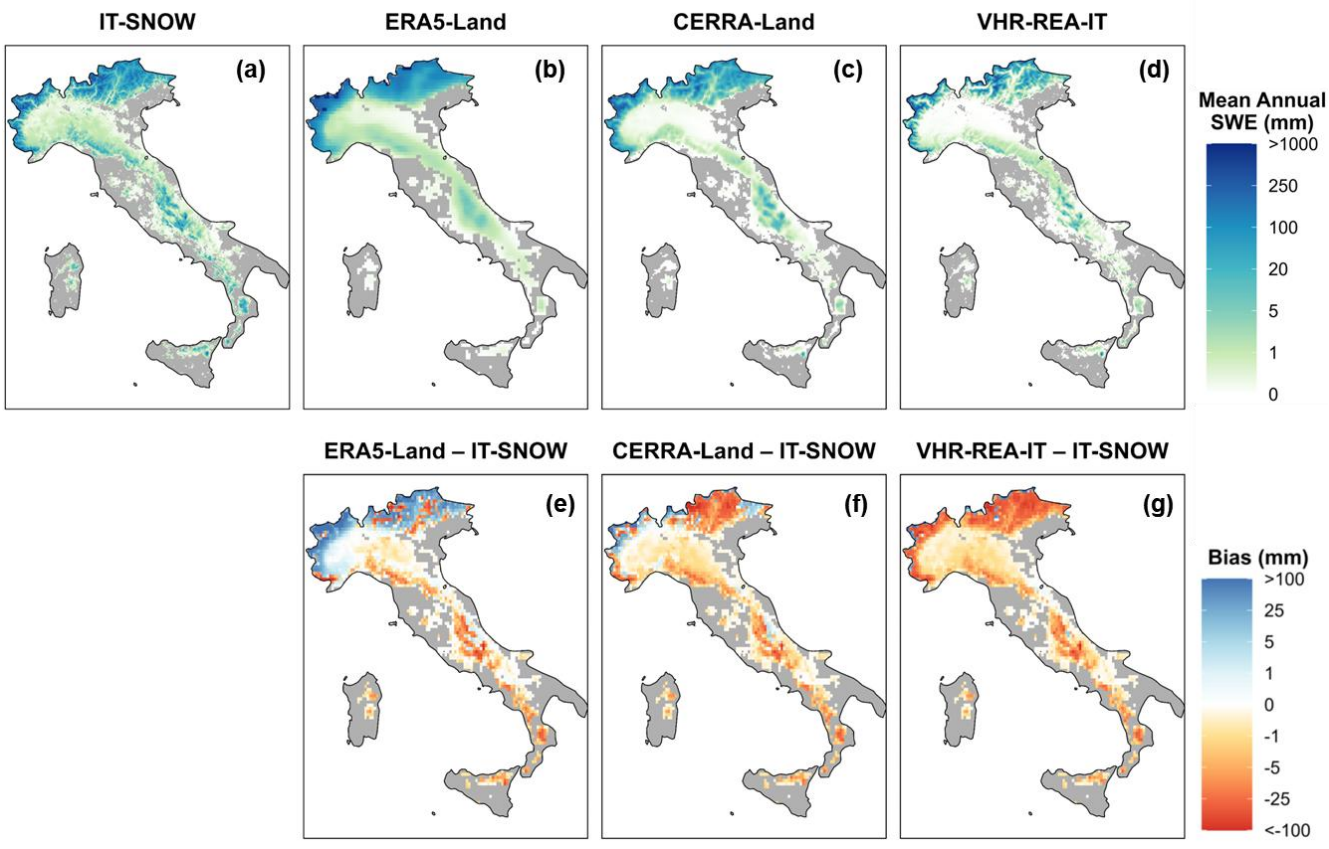

Figure 3. Comparison of mean annual snow water equivalent (SWE) for the period September 2010–August 2024. (a–d) Mean annual SWE maps for the IT-SNOW reference dataset and the three land-surface products at their native resolutions. (e–g) Spatial bias maps (Product – IT-SNOW) resampled to the common 9 km grid.

Looking at this figure, several key patterns can be appreciated. All the datasets (top panels a–d) confirm overall the expected elevation-dependent distribution of snow water equivalent, with highest accumulations concentrated in the high Alpine regions of northern Italy and the Apennine spine. On the other hand, significant differences are observed among the products (highlighted by bias in mean annual SWE, see panels e–g), especially at high elevations where the largest SWE values occur.

Considering the mean annual SWE estimates in more detail, the coarse spatial resolution of ERA5-Land appears to limit its ability to capture the high spatial variability of SWE across the study area (panel b). Besides, the bias map (panel e) shows large positive biases over much of the high Alpine region, alongside some localised negative values, whereas the Apennines and lowlands show widespread underestimation. This tendency for ERA5-Land to overestimate SWE at high Alpine elevations

https://doi.org/10.5194/egusphere-2026-2484
Preprint. Discussion started: 20 May 2026

is consistent with findings from other mountainous regions: for example, Kouki et al. (2023) reported that ERA5-Land overestimates total Northern Hemisphere SWE by 150–200 % in spring, mainly because of very high SWE values in major mountain regions. In the Alps, particularly in the north-western and central sectors, the comparison of the meteorological forcing indicates positive winter precipitation biases together with negative winter temperature biases for ERA5-Land (Fig. B1, panel b), in agreement with Cavalleri et al. (2024a, b), Dalla Torre et al. (2024), and Sarigil et al. (2024). Together, these winter biases favour enhanced snow accumulation, with subsequent persistence into spring. The seasonal analysis (Fig. B1) shows that this pattern is already established during the accumulation season, particularly in the north-western Alps, where autumn–winter precipitation excess coincides with colder-than-observed conditions. The resulting SWE overestimation is therefore consistent with biases established during the accumulation period and maintained into spring (Fig. B1, panels i–k). In the Apennines, the interpretation is less straightforward. In the northern Apennines, the negative SWE bias is mainly consistent with precipitation deficit rather than due to temperature impacts: both autumn and winter precipitation are underestimated, limiting snow accumulation since the onset of the season, whereas later anomalies are too weak or too late to offset the winter deficit (Fig. B1, panels a–d). In the central Apennines, however, forcing biases alone do not fully explain the negative SWE bias. Winter precipitation is near neutral to weakly positive, while temperatures remain below the reference during winter, conditions that would be expected to favour rather than suppress snow accumulation. This suggests that additional factors, such as land-surface model physics or snow parameterisation, also contribute to the simulated deficit.

CERRA-Land demonstrates an improvement in reproducing the spatial variability of mean annual SWE compared to ERA5-Land, attributable to its higher 5.5 km resolution (Fig. 3, panel c). However, despite this improved spatial detail, annual SWE remains negatively biased in most regions, with some localised exceptions (panel f). In the Alps, unlike ERA5-Land which produces marked overestimation due to the combined and uniform strong precipitation and temperature biases, CERRA-Land SWE is influenced by an overall weak underestimation of temperature during snow season (Fig. B2, panels e–g) and a much more varying pattern of precipitation biases (Fig. B2, panels a–d). In the central and eastern Alps, autumn precipitation bias is scattered and changes across the valleys (Fig. B2, panel a), while in winter it is overall weakly negative (Fig. B2, panel b). Such forcing pattern partially explains the strong negative SWE bias in the same region. This suggests that the observed deficit may reflect not only forcing errors but also processes internal to the snow modelling chain, although dedicated process-level diagnostics would be required to identify the specific mechanisms involved. The main Alpine exception is the north-western Alps, where positive autumn–winter precipitation biases (Fig. B2, panels a–b) and colder conditions (Fig. B2, panels e–f) shift the regional mean SWE bias into positive values, although the cell-level pattern remains heterogeneous. However, interpretation of the SWE pattern in areas very close to the national border should nevertheless remain cautious since the reference datasets are less robust: IT-SNOW assimilates fewer observations there (Avanzi et al., 2023), and SCIA does not extend beyond the national border; in addition, gauge station density is also limited in such high-elevation areas. Across the Apennine chain, instead, the attribution is more direct: precipitation deficit is strongest during autumn and winter, leading to

https://doi.org/10.5194/egusphere-2026-2484
Preprint. Discussion started: 20 May 2026

negative SWE biases during the main accumulation season despite the overall weak cold bias, especially in the north. The negative SWE bias is therefore directionally consistent with the precipitation deficit.

VHR-REA_IT exhibits the most spatially widespread negative SWE biases among the evaluated products, despite having the highest spatial resolution (~2.2 km) (Fig. 3, panels d and g). A strong negative SWE bias characterises much of the domain, although some high-elevation Alpine areas show locally positive anomalies during the early accumulation season (Fig. B3, panels i–j). The joint seasonal analysis reveals a seasonal asymmetry in the temperature bias, with a cold bias in winter transitioning to a strong warm bias in summer (Fig. B3, panels f and h), consistent with documented evaluations of the COSMO-CLM atmospheric fields over Italy (Adinolfi et al., 2023; Cavalleri et al., 2024a; Loprieno et al., 2024; Raffa et al., 2021). However, the seasonal meteorological forcing does not fully account for the SWE underestimation in several subregions. In the Alps, winter precipitation is generally overestimated and winter temperatures are colder than the reference (Fig. B3, panels b and f), conditions that should favour snow accumulation, yet SWE bias remains negative in all three Alpine subregions. Similarly, in the central Apennines, precipitation becomes weakly positive in winter while temperatures remain below the reference, yet SWE bias remains negative during the accumulation season (Fig. B3, panels i–k). Only in the northern Apennines do autumn–winter precipitation deficits provide a more direct explanation, although the persistence of negative SWE bias beyond winter suggests that precipitation deficit alone is insufficient to explain the full anomaly. The persistence of negative SWE biases under autumn–winter forcing conditions that would otherwise favour snow accumulation points to structural factors in the modelling chain. Unlike ERA5-Land and CERRA-Land, which are offline simulations driven by observationally constrained reanalysis forcing, VHR-REA_IT is a free-running dynamical downscaling in which COSMO-CLM and its land-surface scheme TERRA-ML operate as a fully coupled atmosphere–land system (Raffa et al., 2021), with no observations assimilated within the regional domain. Any initial negative SWE perturbation generated within this configuration, whether originating in the snow scheme structure, in model parameters, or in the internal forcing, can then be reinforced rather than corrected by the coupled atmosphere and land components: a reduction in simulated SWE lowers surface albedo, warms the lower boundary layer, and promotes further melt through land-atmosphere feedbacks (Santanello et al., 2018) that are not represented in the same two-way form in the offline configurations of the other two products.

5.2 Snow cover duration

Beyond mean annual SWE magnitudes, snow cover duration (SCD), defined in Sect. 4.1 as the mean annual number of days with SWE exceeding 5 mm, provides complementary insights into snowpack temporal dynamics. In fact, SCD helps to better capture the integrated effects of meteorological and topographic factors, including temperature regimes, precipitation patterns, elevation, and energy balance processes, that collectively determine snow persistence. As a diagnostic variable, we used SCD for assessing the performance of the evaluated products across the complete seasonal cycle, as it integrates cumulative effects of biases in both accumulation and melting processes that may not be evident in mean SWE comparisons. Analogously to Fig.

https://doi.org/10.5194/egusphere-2026-2484
Preprint. Discussion started: 20 May 2026

3, Fig. 4 presents the spatial distribution of mean annual SCD for each dataset (panels a–d) at their native resolution and the corresponding biases relative to IT-SNOW (panels e–g) on the common resampled 9 km grid.

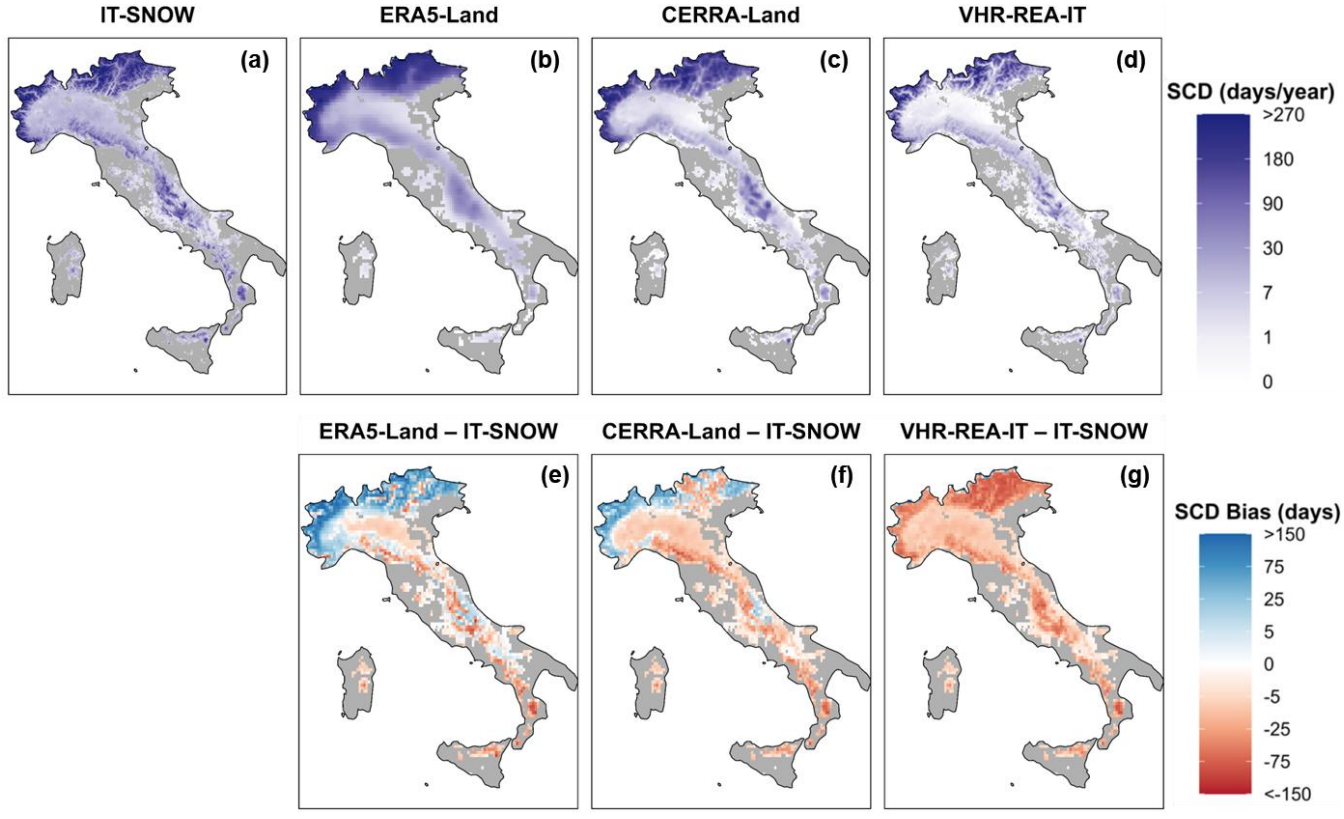

425 **Figure 4. Comparison of mean annual snow cover duration (SCD) for the period September 2010–August 2024. (a–d) Mean annual SCD maps for the IT-SNOW reference dataset and the three land-surface products at their native resolutions. (e–g) Spatial bias maps (Product – IT-SNOW) showing the difference in SCD in days with common 9 km grid.**

The SCD maps (Fig. 4, top panels a–d) confirm a common elevation-dependent spatial pattern along the country, consistent with mean annual SWE in Fig. 3. However, the bias analysis (bottom panels e–g) shows patterns that differ partially from the
430 mean annual SWE biases (Fig. 3), indicating that biases in total snow mass do not always correspond to biases in snow cover persistence.

ERA5-Land (panel e) displays a spatially heterogeneous SCD bias pattern that broadly mirrors the mean annual SWE biases (Fig. 3, panel e), with overestimation over the Alpine region and predominantly negative biases across the Apennines and southern Italy. Over the Alps, the positive SCD bias is the strongest and most spatially coherent in the north-western sector,
435 extending across the high-elevation areas where mean annual SCD is already longest, and weakens progressively towards the central and eastern sectors. This overestimation is consistent with the broader literature, which identifies prolonged snow cover as a characteristic bias of ERA5-Land over high mountain areas (Kouki et al., 2023; Monteiro and Morin, 2023). Over the

https://doi.org/10.5194/egusphere-2026-2484
Preprint. Discussion started: 20 May 2026

European Alps specifically, Monteiro and Morin (2023) found ERA5-Land exhibiting the strongest and most spatially extensive SCD overestimation among all evaluated datasets when compared against MODIS satellite observations, with the largest discrepancies occurring at the melt-out date. Urraca and Gobron (2023), evaluating ERA5-Land against ground stations in the Northern Hemisphere, attributed the systematic positive SCD bias to the tendency of the CHTESSEL land-surface model to overestimate snow depth, likely due to excessive snowfall in the forcing. As discussed in Sect. 5.1, the combination of overestimated precipitation and persistent temperature underestimation over this region inflates both snow accumulation and snow persistence, and the SCD overestimation confirms that these forcing biases translate into prolonged snow cover seasons. In the Apennines, SCD biases are predominantly negative but vary across subregions. The northern Apennines show the most widespread underestimation, consistent with the autumn and winter precipitation deficits identified for these sectors in Sect. 5.1, which limit the number of days on which SWE exceeds the 5 mm threshold and thus shorten the simulated snow season. A similarly widespread negative SCD bias is observed across the southern Apennines. The central Apennines display a more mixed pattern: although mean annual SWE is underestimated across this subregion, a notable fraction of cells exhibits locally positive SCD biases, likely due to the winter and spring weak but persistent cold bias (Fig. B1, panels f–g) that favours snow retention.

CERRA-Land shows a more moderate Alpine SCD overestimation than ERA5-Land, while maintaining negative biases across the Apennines. With the exception of some valleys in the central-eastern Alps, where the product underestimates SCD, most of the Alps show positive SCD bias, with the strongest and most spatially coherent overestimation occurring over the north-western portion of the chain, near the Swiss and French borders. This pattern aligns with the findings of Monteiro and Morin (2023), who reported that CERRA-Land particularly overestimates SCD over the western Italian Alps when compared against MODIS satellite observations. As discussed in Sect. 5.1, this subregion represents a notable exception to the general pattern, with seasonal precipitation overestimated throughout the year alongside a persistent cold bias, conditions that favour both excessive accumulation and prolonged snow retention. Over the most eastern Alps, the positive SCD bias is weaker but still present, consistent with the comparatively modest annual SWE biases in these sectors. Across all three Apennine subregions and southern Italy, CERRA-Land underestimates SCD, with the strongest negative bias in the northern Apennines, consistent with the most severe precipitation deficits in the snow accumulation season identified in Sect. 5.1 (Fig. B2, panels a and b). In the central and southern Apennines, negative SCD biases follow the same attribution discussed for mean annual SWE: autumn and winter precipitation is underestimated while the positive bias is concentrated in the warmer seasons.

VHR-REA_IT (panel g) underestimates SCD across all subregions in both the Alps and the Apennines. Unlike ERA5-Land and CERRA-Land, which show opposing SCD bias signs between the Alps and the Apennines, VHR-REA_IT is the only product with consistently negative SCD biases across all subregions. Within the Alps, the underestimation intensifies from the north-western sector towards the central and eastern sectors, where the SCD deficit is the largest among all subregions despite winter precipitation overestimation and cold temperature biases (Fig. B3, panels b and f), reinforcing the hypothesis that the

https://doi.org/10.5194/egusphere-2026-2484
Preprint. Discussion started: 20 May 2026

attribution may be found in the snow model structure or parameters, as discussed for mean annual SWE. Overall, VHR-REA_IT exhibits the poorest SCD performance among the three evaluated products.

5.3 Temporal correlation of daily SWE

To complement the assessment of annual snowpack characteristics, we evaluated how well each product reproduces the day-to-day variability of SWE through temporal correlation analysis. The Pearson correlation coefficient (r) was calculated at each grid cell between the daily SWE time series of each product and of the IT-SNOW reference, for the entire study period (September 2010–August 2024), following resampling to the common ERA5-Land 9 km spatial resolution. The results are presented in Fig. 5, which displays spatial maps of the correlation coefficients, providing a direct visual assessment of temporal correspondence between simulated and reference snowpack dynamics across Italy.

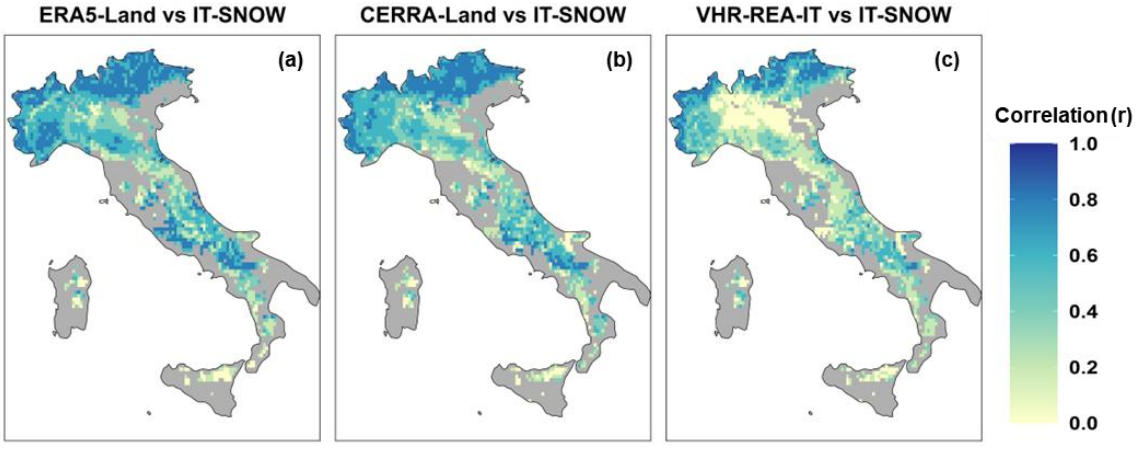

Figure 5. Temporal correlation of daily snow water equivalent (SWE) between each evaluated product and the IT-SNOW reference for the period September 2010–August 2024. The maps display the Pearson correlation coefficient (*r*) for (a) ERA5-Land, (b) CERRA-Land, and (c) VHR-REA_IT with common grid at 9 km resolution.

Overall, ERA5-Land demonstrates the highest daily correlations among the three products, with the strongest agreement in the Alpine region and weaker but still comparatively better performance in the Apennines. Despite the substantial overestimation of SWE magnitude at higher elevations documented in Sect. 5.1, the temporal variability of the simulated snowpack remains broadly consistent with the reference, particularly in the Alps. This is consistent with the offline product architecture described in Sect. 3.2.1: as ERA5's atmospheric data assimilation constrains the sequence and timing of synoptic weather events, the forcing inherited by CHTESSEL is expected to preserve realistic temporal patterns even where simulated mean annual SWE and SCD are biased at the land surface. Similar behaviour has been reported in other mountainous regions, where ERA5-Land maintains reasonable temporal consistency with the reference despite substantial magnitude biases: over parts of Iran, ERA5-Land preserves temporal consistency while overestimating snow depth (Majidi et al., 2025), and over parts of Canada it does so while underestimating SWE (Kanda and Fletcher, 2024).

https://doi.org/10.5194/egusphere-2026-2484
Preprint. Discussion started: 20 May 2026

CERRA-Land shows daily correlation patterns broadly comparable to ERA5-Land across the Alpine region, with similar spatial structure and only slightly lower coefficients in the north-western sector. In the Apennines, however, the correlation weakens more substantially than for ERA5-Land, particularly in the northern sector. This stronger degradation is consistent with the more severe autumn and winter precipitation deficits in CERRA-Land's forcing over the Apennines discussed in Sect. 5.1 (Fig. B2, panels a and b), which exceed those of ERA5-Land in the same subregions. In these lower-elevation Apennine regions, where snow cover is more intermittent, such deficits are more likely to reduce the simulated duration and continuity of snow cover during periods when the reference indicates snow presence, thereby affecting not only snow amount but also snow persistence and weakening the temporal correspondence of daily SWE with the reference time series.

VHR-REA_IT exhibits markedly poorer performance in capturing daily SWE dynamics, with substantially lower daily correlations throughout most of Italy, particularly in the Apennines and at lower elevations, where coefficients often fall below 0.4. This weak temporal correspondence is consistent with VHR-REA_IT's systematic underestimation of both mean annual SWE and SCD documented in Sections 5.1 and 5.2. The severe underestimation of SWE produces frequent zero or near-zero values when a substantial snowpack should exist, thereby degrading the correlation. Therefore, the model fails to capture day-to-day variability for snow that it incorrectly simulates as absent.

6 Conclusions

This study evaluated SWE estimates from three land-surface land-surface products, ERA5-Land, CERRA-Land, and VHR-REA_IT, against the IT-SNOW reference over Italy using three complementary indicators: mean annual SWE, snow cover duration, and temporal correlation of daily SWE series. To support the interpretation of the identified SWE discrepancies, the analysis also incorporated a complementary evaluation of the products' precipitation and temperature biases relative to the gauge-based national reference SCIA fields. The results show that product performance varies across the different Italian mountain regions and different indications may be drawn from the evaluation metrics. The complementary precipitation and temperature analysis helps to attribute a substantial part of the SWE differences to their meteorological origins, although in some regions and products the forcing biases alone do not fully account for the SWE discrepancies.

Among the three products, ERA5-Land showed the strongest positive biases in mean annual SWE and snow cover duration in the Alpine domain, especially in the north-western and central Alps, where precipitation overestimation and persistent cold biases favour both excessive accumulation and prolonged snow persistence. In the Apennines, by contrast, ERA5-Land generally underestimated both mean SWE and snow cover duration, consistent with autumn and winter precipitation deficits that limit snow accumulation. Despite these magnitude biases, ERA5-Land achieved the strongest temporal correlations with IT-SNOW daily time series, indicating that it reproduces day-to-day snowpack variability more faithfully than the other products. CERRA-Land reproduced spatial SWE patterns in more detail than ERA5-Land due to its finer resolution, but still underestimated mean SWE across most analysed subregions, with the main exception of the north-western Alps. In the central and eastern Alps, CERRA-Land exhibits negative mean annual SWE bias alongside positive SCD bias, suggesting that the

https://doi.org/10.5194/egusphere-2026-2484
Preprint. Discussion started: 20 May 2026

snowpack, while smaller in total mass, persists longer than indicated by the reference. This is consistent with the persistent cold bias across the snow season in these subregions, which may delay melt onset and extend the snow-covered period even where accumulation is limited by a weak underestimation of winter precipitation. In the Apennines, CERRA-Land showed broadly negative mean SWE and SCD biases, with the strongest deficits in the northern Apennines. VHR-REA_IT exhibited the poorest overall performance, with the most spatially widespread underestimation of SWE and SCD and the weakest daily correlations. The systematic underestimation of snow mass is the central limitation: by reducing the simulated snowpack, it shortens the snow-covered period and introduces prolonged mismatches with the reference time series, which in turn degrade the temporal correspondence. The results suggest that these limitations are consistent with the absence of observational assimilation within the regional domain: unlike ERA5-Land and CERRA-Land, whose forcing fields inherit observational constraints from their parent atmospheric reanalyses, VHR-REA_IT meteorological fields evolve freely within its boundaries, leaving biases generated during the simulation uncorrected. A full understanding of the remaining discrepancies will require dedicated process-level and sensitivity analyses to isolate the respective roles of forcing, snow model structure, and coupled land–atmosphere feedbacks, which are beyond the scope of this work.

A central motivation of this study was to assess whether any of the evaluated products could be reliably used for extending SWE information beyond the relatively short IT-SNOW period. In this respect, ERA5-Land appears to be the most promising candidate, not so much because it provides the most accurate snow magnitudes, but because it shows the highest temporal fidelity across much of the domain. This may support applications focused on interannual variability, anomaly detection, or standardised snow indices, provided that the consistency of bias characteristics over time is carefully assessed, and systematic biases are accounted for, before its use in long-term hydro-climatological analyses. CERRA-Land also shows potential, particularly in parts of the Alpine domain, but its performance over the entirety of Italy appears limited by the quality of precipitation forcing. Given that CERRA-Land precipitation is refined through the MESCAN analysis system, the contrast between the present results and more favourable findings reported elsewhere in Europe (Monteiro and Morin, 2023) suggests that the gauge density of the assimilated precipitation plays an important role in controlling its added value. VHR-REA_IT, in its current form, does not provide a sufficiently reliable basis for record extension, although its convection-permitting resolution and fully coupled architecture represent a physically more ambitious framework than the offline configurations of the other two products; realising this potential would likely require the incorporation of observational constraints within the regional domain.

More broadly, this study shows that evaluating SWE products jointly with the meteorological fields that drive the snow accumulation and melt modelling allows a more comprehensive interpretation of their differences and of the performance indicators, since it helps to distinguish where SWE biases are primarily consistent with forcing errors and where additional factors related to snow process representation are likely involved. This provides a transferable evaluation framework for other regions where benchmark snow datasets are available for a limited period only.

https://doi.org/10.5194/egusphere-2026-2484
Preprint. Discussion started: 20 May 2026

Appendices

Appendix A: Mean annual precipitation and temperature biases

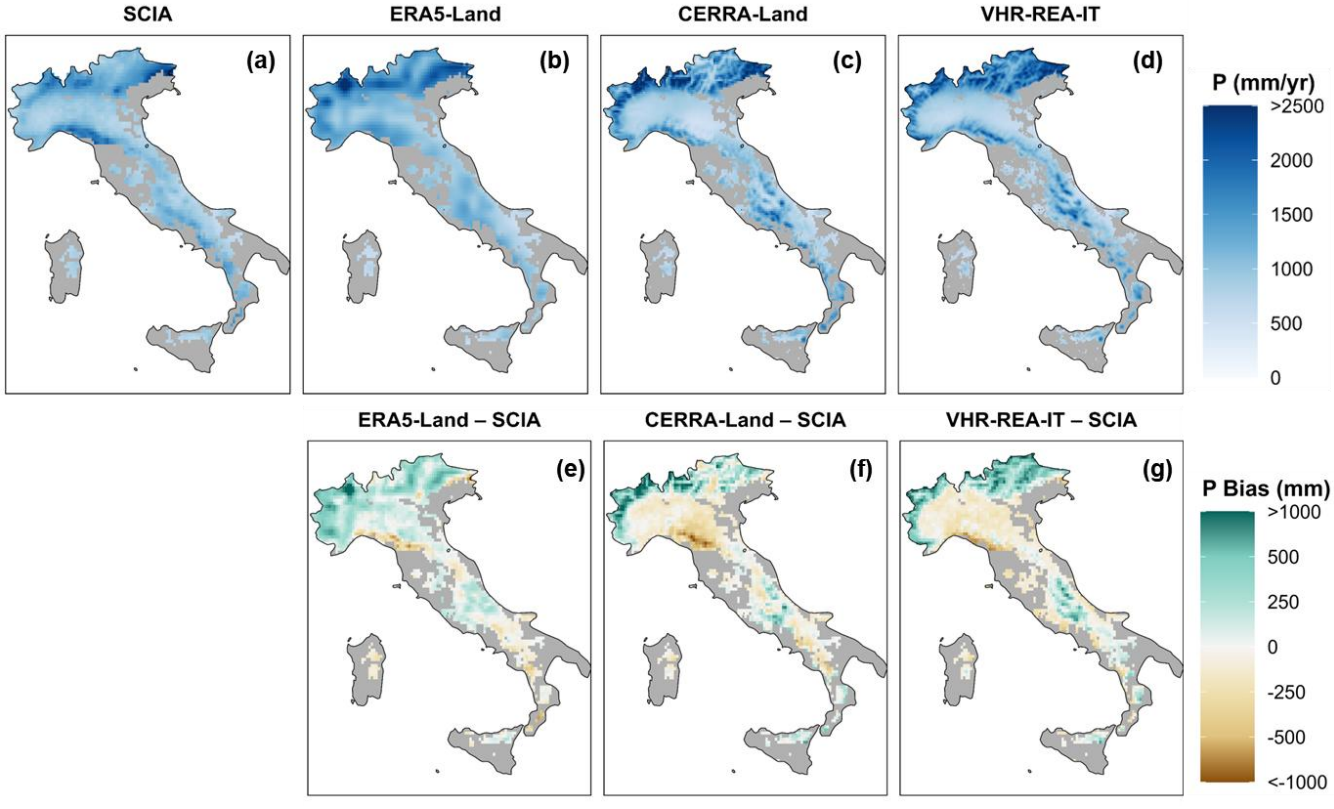

Figure A1. Comparison of mean annual precipitation for the period September 2010–August 2024. (a–d) Mean annual precipitation maps for the SCIA reference dataset and the three land-surface products (ERA5-Land, CERRA-Land, VHR-REA_IT) at their native resolutions. (e–g) Spatial bias maps (Product – SCIA) showing the difference in precipitation between each of the three land-surface products and the reference dataset, resampled to a common 9 km grid. Positive values indicate overestimation; negative values indicate underestimation.

https://doi.org/10.5194/egusphere-2026-2484
Preprint. Discussion started: 20 May 2026

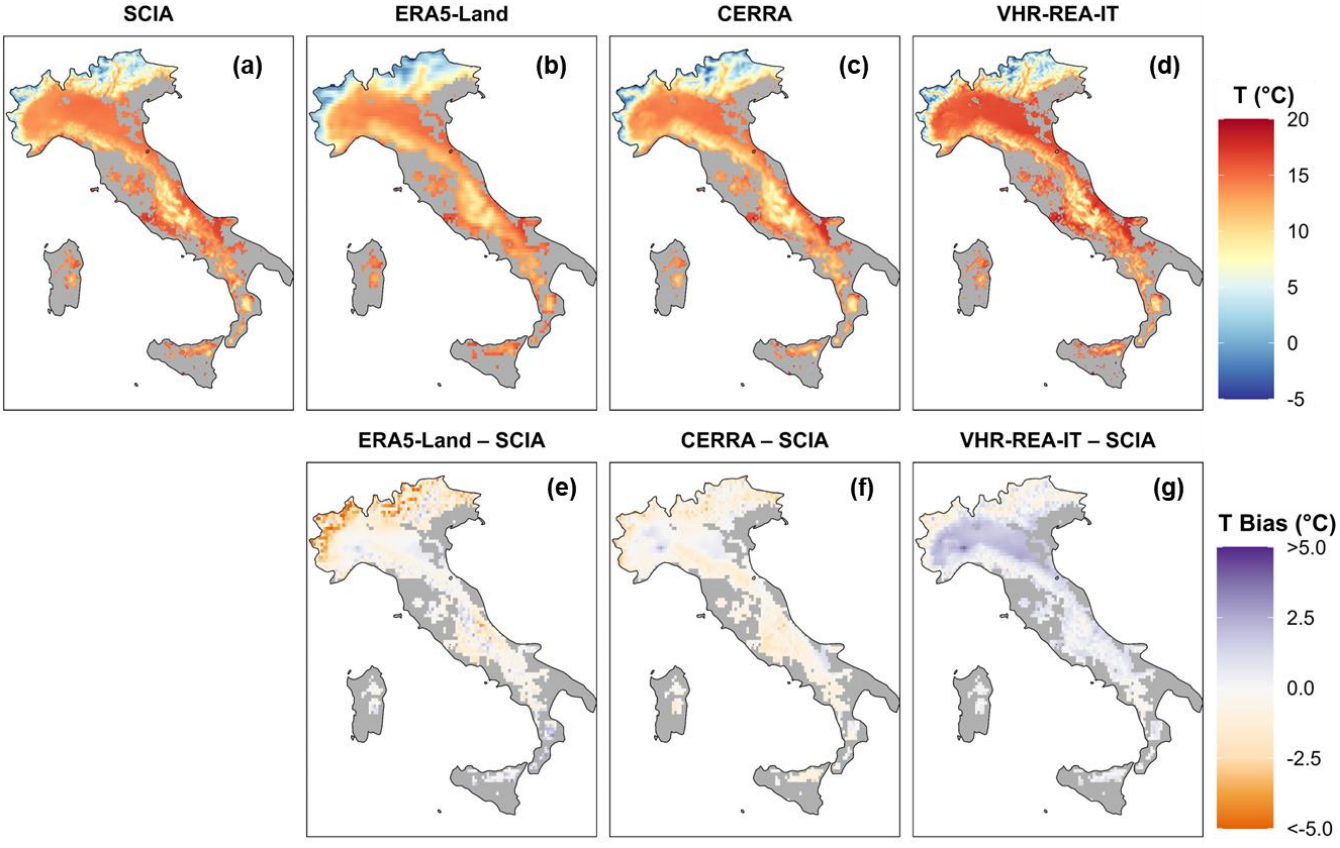

Figure A2. Comparison of mean annual temperature for the period September 2010–August 2024. (a–d) Mean annual temperature maps for the SCIA reference dataset and three land-surface products (ERA5-Land, CERRA-Land, VHR-REA_IT) at their native resolutions. (e–g) Spatial bias maps (Product – SCIA) showing the difference in temperature between each of the three land-surface products and the reference dataset, resampled to a common 9 km grid. Positive values indicate warm bias; negative values indicate cold bias.

https://doi.org/10.5194/egusphere-2026-2484
Preprint. Discussion started: 20 May 2026

Appendix B: Mean seasonal biases in precipitation, temperature and SWE

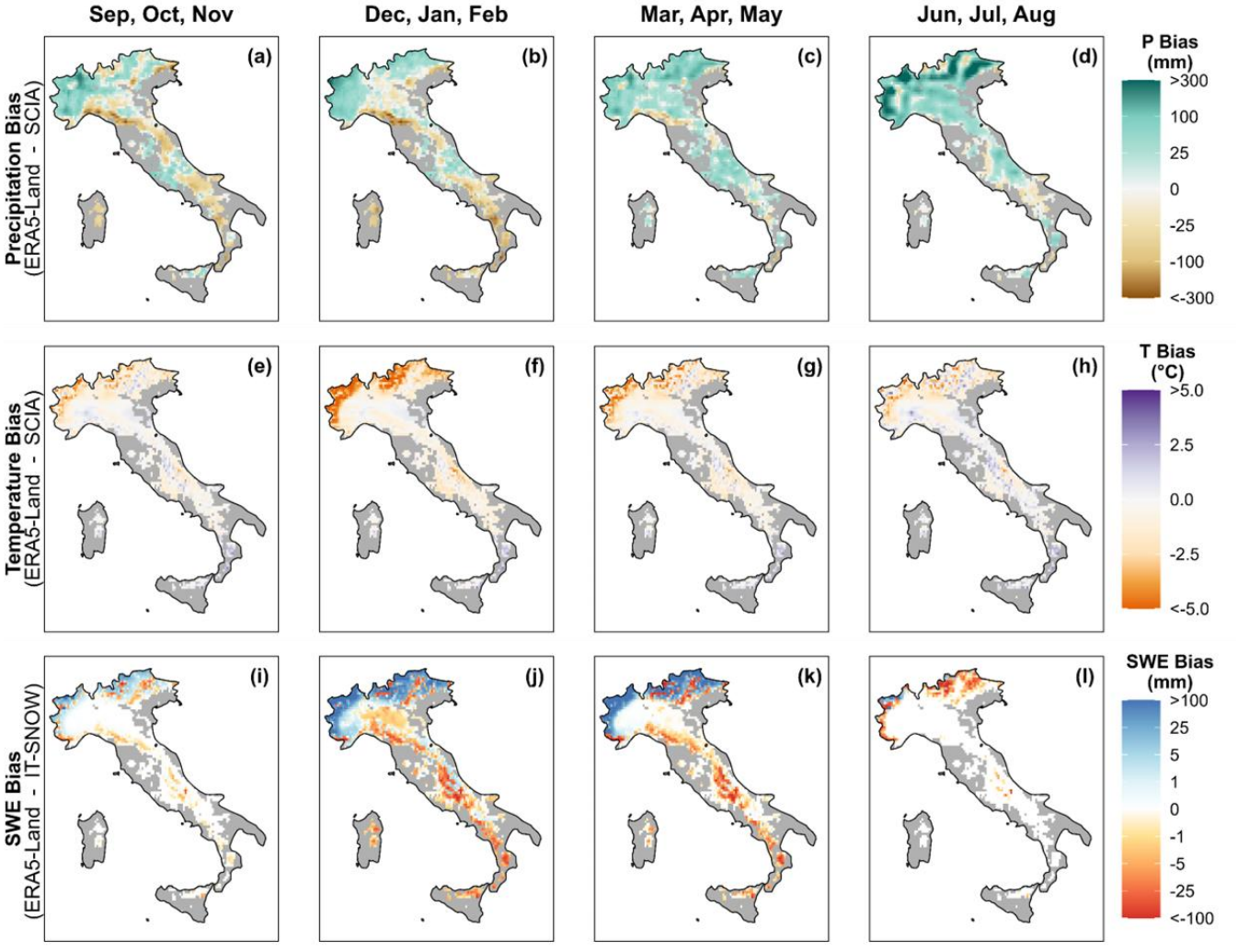

Figure B1. Seasonal biases in precipitation, temperature, and snow water equivalent for ERA5-Land relative to reference datasets (SCIA for precipitation and temperature; IT-SNOW for SWE) for the period September 2010–August 2024. The first row (a–d) shows precipitation bias (ERA5-Land – SCIA), the second row (e–h) shows temperature bias (ERA5-Land – SCIA), and the third row (i–l) shows SWE bias (ERA5-Land – IT-SNOW). Each column represents the calendar season: (a, e, i) Autumn (September–November), (b, f, j) Winter (December–February), (c, g, k) Spring (March–May), and (d, h, l) Summer (June–August). All bias maps are resampled to a common 9 km grid. Positive values indicate overestimation by ERA5-Land; negative values indicate underestimation.

https://doi.org/10.5194/egusphere-2026-2484
Preprint. Discussion started: 20 May 2026

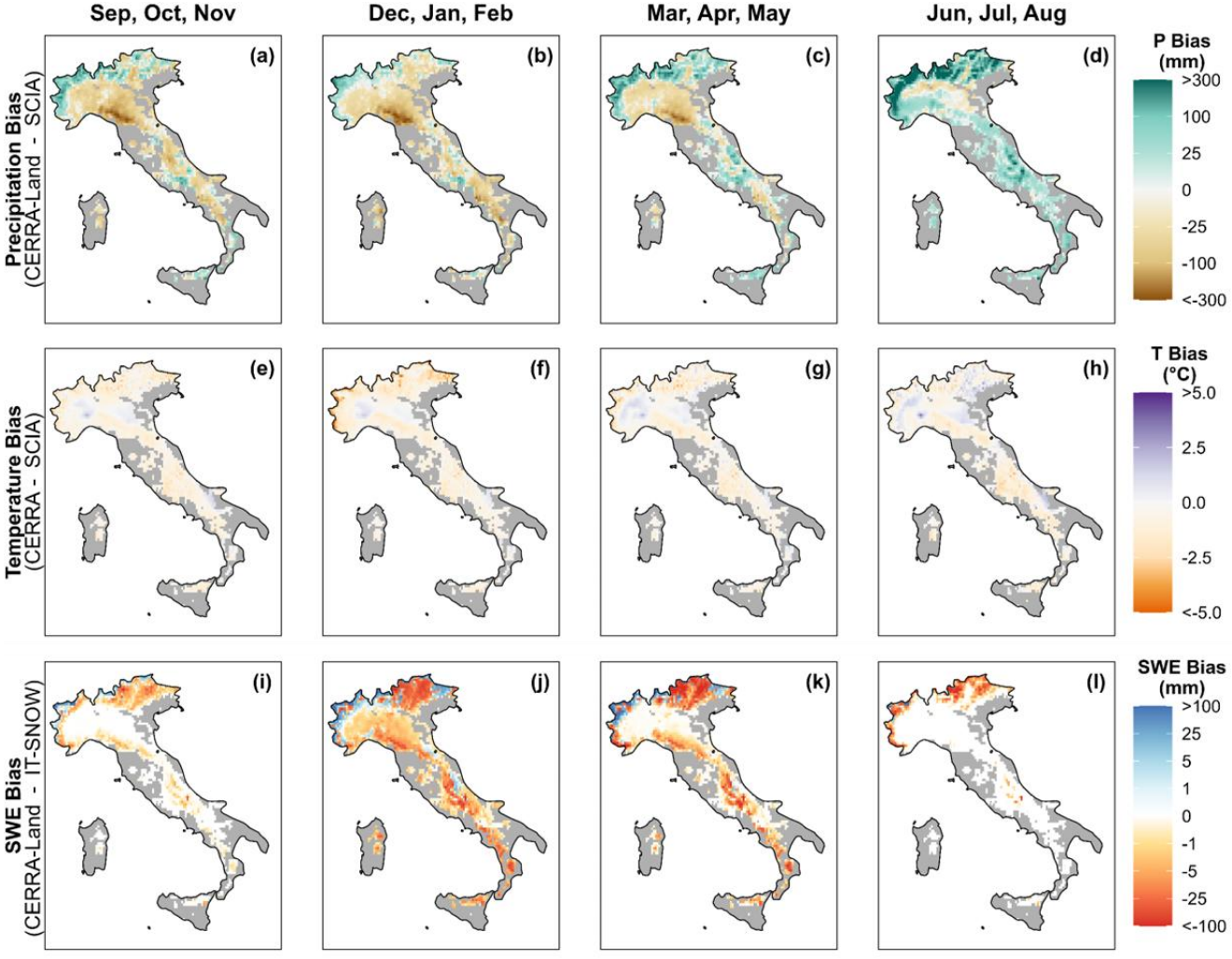

Figure B2. Seasonal biases in precipitation, temperature, and snow water equivalent for CERRA-Land relative to reference datasets (SCIA for precipitation and temperature; IT-SNOW for SWE) for the period September 2010–August 2024. The first row (a–d) shows precipitation bias (CERRA-Land – SCIA), the second row (e–h) shows temperature bias (CERRA – SCIA), and the third row (i–l) shows SWE bias (CERRA-Land – IT-SNOW). Each column represents the calendar season: (a, e, i) Autumn (September–November), (b, f, j) Winter (December–February), (c, g, k) Spring (March–May), and (d, h, l) Summer (June–August). All bias maps are resampled to a common 9 km grid. Positive values indicate overestimation by CERRA-Land; negative values indicate underestimation.

https://doi.org/10.5194/egusphere-2026-2484
Preprint. Discussion started: 20 May 2026

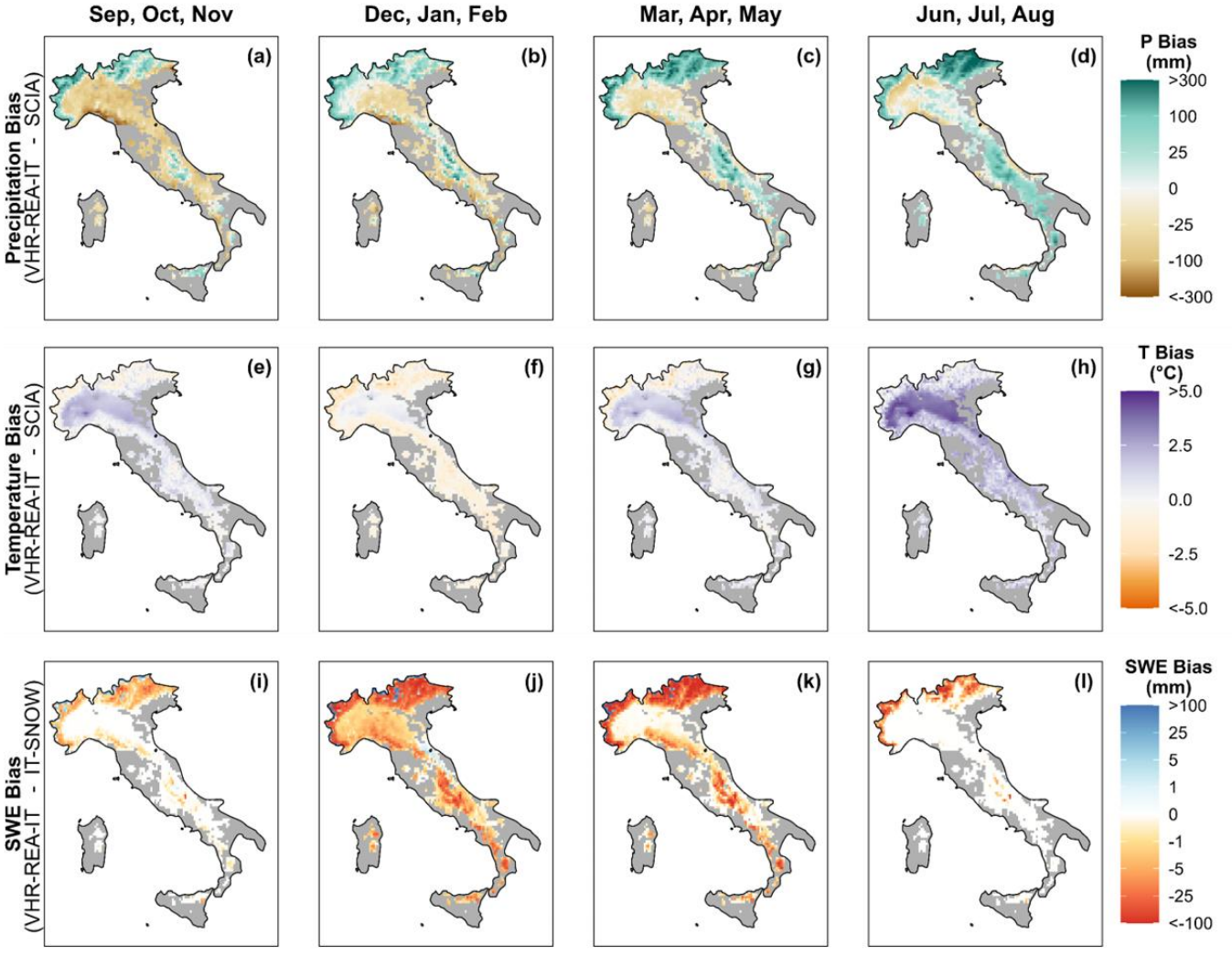

590 **Figure B3. Seasonal biases in precipitation, temperature, and snow water equivalent for VHR-REA_IT relative to reference datasets (SCIA for precipitation and temperature; IT-SNOW for SWE) for the period September 2010–August 2024. The first row (a–d) shows precipitation bias (VHR-REA_IT – SCIA), the second row (e–h) shows temperature bias (VHR-REA_IT – SCIA), and the third row (i–l) shows SWE bias (VHR-REA_IT – IT-SNOW). Each column represents the calendar season: (a, e, i) Autumn (September–November), (b, f, j) Winter (December–February), (c, g, k) Spring (March–May), and (d, h, l) Summer (June–August).**
595 **All bias maps are resampled to a common 9 km grid. Positive values indicate overestimation by VHR-REA_IT; negative values indicate underestimation.**

Data availability

All datasets analysed in this study are publicly available from their respective providers.

https://doi.org/10.5194/egusphere-2026-2484
Preprint. Discussion started: 20 May 2026

Author contribution

GS: conceptualization, data curation, formal analysis, investigation, methodology, validation, visualization, writing – original draft, writing – review and editing. MN: conceptualization, investigation, methodology, validation, supervision, writing – review and editing. FA: supervision, writing – review and editing. ET: conceptualization, investigation, methodology, resources, validation, supervision, writing – review and editing.

Competing interests

At least one of the co-authors is a member of the editorial board of *Hydrology and Earth System Sciences*. The authors have no other competing interests to declare.

Financial support

This study was carried out within the RETURN Extended Partnership and received funding from the European Union NextGenerationEU (National Recovery and Resilience Plan – NRRP, Mission 4, Component 2, Investment 1.3, D.D. no. 1243 of 2 August 2022, grant no. PE0000005), and within the project "Stochastic amplification of climate change into floods and droughts change (CO2²Water)", funded by the Italian Science Fund under grant no. J53C23003860001.

References

Adinolfi, M., Raffa, M., Reder, A., and Mercogliano, P.: Investigation on potential and limitations of ERA5 Reanalysis downscaled on Italy by a convection-permitting model, Clim Dyn, 61, 4319–4342, https://doi.org/10.1007/s00382-023-06803-w, 2023.

Avanzi, F., Gabellani, S., Delogu, F., Silvestro, F., Cremonese, E., Morra di Cella, U., Ratto, S., and Stevenin, H.: Snow Multidata Mapping and Modeling (S3M) 5.1: a distributed cryospheric model with dry and wet snow, data assimilation, glacier mass balance, and debris-driven melt, Geoscientific Model Development, 15, 4853–4879, https://doi.org/10.5194/gmd-15-4853-2022, 2022.

Avanzi, F., Gabellani, S., Delogu, F., Silvestro, F., Pignone, F., Bruno, G., Pulvirenti, L., Squicciarino, G., Fiori, E., Rossi, L., Puca, S., Toniazzo, A., Giordano, P., Falzacappa, M., Ratto, S., Stevenin, H., Cardillo, A., Fioletti, M., Cazzuli, O., Cremonese, E., Morra di Cella, U., and Ferraris, L.: IT-SNOW: a snow reanalysis for Italy blending modeling, in situ data, and satellite observations (2010–2021), Earth System Science Data, 15, 639–660, https://doi.org/10.5194/essd-15-639-2023, 2023.

Avanzi, F., Munerol, F., Milelli, M., Gabellani, S., Massari, C., Girotto, M., Cremonese, E., Galvagno, M., Bruno, G., Morra di Cella, U., Rossi, L., Altamura, M., and Ferraris, L.: Winter snow deficit was a harbinger of summer 2022 socio-hydrologic drought in the Po Basin, Italy, Commun Earth Environ, 5, 64, https://doi.org/10.1038/s43247-024-01222-z, 2024.

Baatz, R., Hendricks Franssen, H. J., Euskirchen, E., Sihi, D., Dietze, M., Ciavatta, S., Fennel, K., Beck, H., De Lannoy, G., Pauwels, V. R. N., Raiho, A., Montzka, C., Williams, M., Mishra, U., Poppe, C., Zacharias, S., Lausch, A., Samaniego, L., Van Looy, K., Bogena, H., Adamescu, M., Mirtl, M., Fox, A., Goergen, K., Naz, B. S., Zeng, Y., and Vereecken, H.: Reanalysis in Earth System Science: Toward Terrestrial Ecosystem Reanalysis, Reviews of Geophysics, 59, e2020RG000715, https://doi.org/10.1029/2020RG000715, 2021.

https://doi.org/10.5194/egusphere-2026-2484
Preprint. Discussion started: 20 May 2026

Bales, R. C., Molotch, N. P., Painter, T. H., Dettinger, M. D., Rice, R., and Dozier, J.: Mountain hydrology of the western United States, Water Resources Research, 42, https://doi.org/10.1029/2005WR004387, 2006.

Balsamo, G., Beljaars, A., Scipal, K., Viterbo, P., Hurk, B. van den, Hirschi, M., and Betts, A. K.: A Revised Hydrology for the ECMWF Model: Verification from Field Site to Terrestrial Water Storage and Impact in the Integrated Forecast System, Journal of Hydrometeorology, 10, 623–643, https://doi.org/10.1175/2008JHM1068.1, 2009.

Barnett, T. P., Adam, J. C., and Lettenmaier, D. P.: Potential impacts of a warming climate on water availability in snow-dominated regions, Nature, 438, 303–309, https://doi.org/10.1038/nature04141, 2005.

Bengtsson, L., Andrae, U., Aspelien, T., Batrak, Y., Calvo, J., Rooy, W. de, Gleeson, E., Hansen-Sass, B., Homleid, M., Hortal, M., Ivarsson, K.-I., Lenderink, G., Niemelä, S., Nielsen, K. P., Onvlee, J., Rontu, L., Samuelsson, P., Muñoz, D. S., Subias, A., Tijm, S., Toll, V., Yang, X., and Køltzow, M. Ø.: The HARMONIE–AROME Model Configuration in the ALADIN–HIRLAM NWP System, Monthly Weather Review, 145, 1919–1935, https://doi.org/10.1175/MWR-D-16-0417.1, 2017.

Betts, A. K., Ball, J. H., Beljaars, A. C. M., Miller, M. J., and Viterbo, P. A.: The land surface-atmosphere interaction: A review based on observational and global modeling perspectives, Journal of Geophysical Research: Atmospheres, 101, 7209–7225, https://doi.org/10.1029/95JD02135, 1996.

Bocchiola, D. and Diolaiuti, G.: Evidence of climate change within the Adamello Glacier of Italy, Theor Appl Climatol, 100, 351–369, https://doi.org/10.1007/s00704-009-0186-x, 2010.

Boone, A. and Etchevers, P.: An Intercomparison of Three Snow Schemes of Varying Complexity Coupled to the Same Land Surface Model: Local-Scale Evaluation at an Alpine Site, Journal of Hydrometeorology, 2, 374–394, https://doi.org/10.1175/1525-7541(2001)002%3C0374:AIOTSS%3E2.0.CO;2, 2001.

Bormann, K., Brown, R., Derksen, C., and Painter, T.: Estimating snow-cover trends from space, Nature Climate Change, 8, https://doi.org/10.1038/s41558-018-0318-3, 2018.

Brown, R., Tapsoba, D., and Derksen, C.: Evaluation of snow water equivalent datasets over the Saint-Maurice river basin region of southern Québec, Hydrological Processes, 32, 2748–2764, https://doi.org/10.1002/hyp.13221, 2018.

Broxton, P. D., Zeng, X., and Dawson, N.: Why Do Global Reanalyses and Land Data Assimilation Products Underestimate Snow Water Equivalent?, Journal of Hydrometeorology, 17, 2743–2761, https://doi.org/10.1175/jhm-d-16-0056.1, 2016.

Bruno, G., Pignone, F., Silvestro, F., Gabellani, S., Schiavi, F., Rebora, N., Giordano, P., and Falzacappa, M.: Performing Hydrological Monitoring at a National Scale by Exploiting Rain-Gauge and Radar Networks: The Italian Case, Atmosphere, 12, 771, https://doi.org/10.3390/atmos12060771, 2021.

Cavalleri, F., Viterbo, F., Brunetti, M., Bonanno, R., Manara, V., Lussana, C., Lacavalla, M., and Maugeri, M.: Inter-comparison and validation of high-resolution surface air temperature reanalysis fields over Italy, Int. J. Climatol., 44, 2681–2700, https://doi.org/10.1002/joc.8475, 2024a.

Cavalleri, F., Lussana, C., Viterbo, F., Brunetti, M., Bonanno, R., Manara, V., Lacavalla, M., Sperati, S., Raffa, M., Capecchi, V., Cesari, D., Giordani, A., Cerenzia, I. M. L., and Maugeri, M.: Multi-scale assessment of high-resolution reanalysis precipitation fields over Italy, Atmospheric Research, 312, 107734, https://doi.org/10.1016/j.atmosres.2024.107734, 2024b.

Chang, A. T. C., Foster, J. L., and Hall, D. K.: Nimbus-7 SMMR Derived Global Snow Cover Parameters, Annals of Glaciology, 9, 39–44, https://doi.org/10.3189/S0260305500200736, 1987.

Cho, E., Vuyovich, C. M., Kumar, S. V., Wrzesien, M. L., Kim, R. S., and Jacobs, J. M.: Precipitation biases and snow physics limitations drive the uncertainties in macroscale modeled snow water equivalent, Hydrology and Earth System Sciences, 26, 5721–5735, https://doi.org/10.5194/hess-26-5721-2022, 2022.

Courtier, P., Thépaut, J.-N., and Hollingsworth, A.: A strategy for operational implementation of 4D-Var, using an incremental approach, Quarterly Journal of the Royal Meteorological Society, 120, 1367–1387, https://doi.org/10.1002/qj.49712051912, 1994.

Dalla Torre, D., Di Marco, N., Menapace, A., Avesani, D., Righetti, M., and Majone, B.: Suitability of ERA5-Land reanalysis dataset for hydrological modelling in the Alpine region, Journal of Hydrology: Regional Studies, 52, 101718, https://doi.org/10.1016/j.ejrh.2024.101718, 2024.

https://doi.org/10.5194/egusphere-2026-2484
Preprint. Discussion started: 20 May 2026

Dall'Amico, M., Tasin, S., Di Paolo, F., Brian, M., Leoni, P., Tornatore, F., Formetta, G., Wani, J. M., Rigon, R., and Roati, G.: 30-years (1991-2021) Snow Water Equivalent Dataset in the Po River District, Italy, Sci Data, 12, 374, https://doi.org/10.1038/s41597-025-04633-5, 2025.

Dawson, N., Broxton, P., and Zeng, X.: Evaluation of Remotely Sensed Snow Water Equivalent and Snow Cover Extent over the Contiguous United States, Journal of Hydrometeorology, 19, 1777–1791, https://doi.org/10.1175/JHM-D-18-0007.1, 2018.

Decharme, B., Brun, E., Boone, A., Delire, C., Le Moigne, P., and Morin, S.: Impacts of snow and organic soils parameterization on northern Eurasian soil temperature profiles simulated by the ISBA land surface model, The Cryosphere, 10, 853–877, https://doi.org/10.5194/tc-10-853-2016, 2016.

Desiato, F., Lena, F., and Toreti, A.: SCIA: a system for a better knowledge of the Italian climate, Bollettino di Geofisica Teorica ed Applicata, 48, 351–358, 2007.

Desiato, F., Fioravanti, G., Fraschetti, P., Perconti, W., and Toreti, A.: Climate indicators for Italy: calculation and dissemination, Adv. Sci. Res., 6, 147–150, https://doi.org/10.5194/asr-6-147-2011, 2011.

Di Marco, N., Avesani, D., Righetti, M., Zaramella, M., Majone, B., and Borga, M.: Reducing hydrological modelling uncertainty by using MODIS snow cover data and a topography-based distribution function snowmelt model, Journal of Hydrology, 599, 126020, https://doi.org/10.1016/j.jhydrol.2021.126020, 2021.

Doms, G., Förstner, J., Heise, E., Herzog, H.-J., Mironov, D., Raschendorfer, M., Reinhardt, T., Ritter, B., Schrodin, R., Schulz, J.-P., and Vogel, G.: A Description of the Nonhydrostatic Regional COSMO Model, Part II: Physical Parameterization, Consortium for Small-Scale Modelling, Deutscher Wetterdienst, Offenbach, Germany, 161 pp., available at: http://www.cosmo-model.org, 2024.

Dong, J., Walker, J. P., and Houser, P. R.: Factors affecting remotely sensed snow water equivalent uncertainty, Remote Sensing of Environment, 97, 68–82, https://doi.org/10.1016/j.rse.2005.04.010, 2005.

Dutra, E., Stepanenko, V., Balsamo, G., Viterbo, P., Miranda, P., Mironov, D., and Schaer, C.: An offline study of the impact of lakes on the performance of the ECMWF surface scheme, Boreal environment research, 15, 100–112, 2010.

Essery, R., Morin, S., Lejeune, Y., and B Ménard, C.: A comparison of 1701 snow models using observations from an alpine site, Advances in Water Resources, 55, 131–148, https://doi.org/10.1016/j.advwatres.2012.07.013, 2013.

Frei, C. and Schär, C.: A precipitation climatology of the Alps from high-resolution rain-gauge observations, International Journal of Climatology, 18, 873–900, https://doi.org/10.1002/(SICI)1097-0088(19980630)18:8%3C873::AID-JOC255%3E3.0.CO;2-9, 1998.

Froidurot, S., Zin, I., Hingray, B., and Gautheron, A.: Sensitivity of Precipitation Phase over the Swiss Alps to Different Meteorological Variables, Journal of Hydrometeorology, 15, 685–696, https://doi.org/10.1175/JHM-D-13-073.1, 2014.

Giorgi, F. and Mearns, L. O.: Introduction to special section: Regional climate modeling revisited, J. Geophys. Res.-Atmos., 104, 6335–6352, https://doi.org/10.1029/98JD02072, 1999.

Günther, D., Hanzer, F., Warscher, M., Essery, R., and Strasser, U.: Including Parameter Uncertainty in an Intercomparison of Physically-Based Snow Models, Front. Earth Sci., 8, https://doi.org/10.3389/feart.2020.542599, 2020.

Hall, D. K., Riggs, G. A., Salomonson, V. V., DiGirolamo, N. E., and Bayr, K. J.: MODIS snow-cover products, Remote Sensing of Environment, 83, 181–194, https://doi.org/10.1016/S0034-4257(02)00095-0, 2002.

Hersbach, H., Bell, B., Berrisford, P., Hirahara, S., Horányi, A., Muñoz-Sabater, J., Nicolas, J., Peubey, C., Radu, R., Schepers, D., Simmons, A., Soci, C., Abdalla, S., Abellan, X., Balsamo, G., Bechtold, P., Biavati, G., Bidlot, J., Bonavita, M., De Chiara, G., Dahlgren, P., Dee, D., Diamantakis, M., Dragani, R., Flemming, J., Forbes, R., Fuentes, M., Geer, A., Haimberger, L., Healy, S., Hogan, R. J., Hólm, E., Janisková, M., Keeley, S., Laloyaux, P., Lopez, P., Lupu, C., Radnoti, G., de Rosnay, P., Rozum, I., Vamborg, F., Villaume, S., and Thépaut, J.-N.: The ERA5 global reanalysis, Quarterly Journal of the Royal Meteorological Society, 146, 1999–2049, https://doi.org/10.1002/qj.3803, 2020.

Immerzeel, W. W., Lutz, A. F., Andrade, M., Bahl, A., Biemans, H., Bolch, T., Hyde, S., Brumby, S., Davies, B. J., Elmore, A. C., Emmer, A., Feng, M., Fernández, A., Haritashya, U., Kargel, J. S., Koppes, M., Kraaijenbrink, P. D. A., Kulkarni, A. V., Mayewski, P. A., Nepal, S., Pacheco, P., Painter, T. H., Pellicciotti, F., Rajaram, H., Rupper, S., Sinisalo, A., Shrestha, A. B., Viviroli, D., Wada, Y., Xiao, C., Yao, T., and Baillie, J. E. M.: Importance and vulnerability of the world's water towers, Nature, 577, 364–369, https://doi.org/10.1038/s41586-019-1822-y, 2020.

https://doi.org/10.5194/egusphere-2026-2484
Preprint. Discussion started: 20 May 2026

Jenicek, M., Seibert, J., Zappa, M., Staudinger, M., and Jonas, T.: Importance of maximum snow accumulation for summer low flows in humid catchments, Hydrol. Earth Syst. Sci., 20, 859–874, https://doi.org/10.5194/hess-20-859-2016, 2016

Jenicek, M., Hnilica, J., Nedelcev, O., and Sipek, V.: Future changes in snowpack will impact seasonal runoff and low flows in Czechia, Journal of Hydrology: Regional Studies, 37, 100899, https://doi.org/10.1016/j.ejrh.2021.100899, 2021.

Jones, P. W.: First- and Second-Order Conservative Remapping Schemes for Grids in Spherical Coordinates, Monthly Weather Review, 127, 2204–2210, https://doi.org/10.1175/1520-0493(1999)127%3C2204:FASOCR%3E2.0.CO;2, 1999.

von Kaenel, M. and Margulis, S. A.: Improved modelling of mountain snowpacks with spatially distributed precipitation bias correction derived from historical reanalysis, The Cryosphere, 19, 3309–3327, https://doi.org/10.5194/tc-19-3309-2025, 2025.

Kalnay, E.: Atmospheric Modeling, Data Assimilation and Predictability, Cambridge University Press, 364 pp., 2003.

Kanda, N. and Fletcher, C. G.: Evaluating a hierarchy of bias correction methods for ERA5-Land SWE in northern Canada, EGUsphere, 1–24, https://doi.org/10.5194/egusphere-2024-639, 2024.

Kelly, R.: The AMSR-E snow depth algorithm: Description and initial results, Journal of the Remote Sensing Society of Japan, 29, 307–317, https://doi.org/10.11440/rssj.29.307, 2009.

King, F., Erler, A. R., Frey, S. K., and Fletcher, C. G.: Application of machine learning techniques for regional bias correction of snow water equivalent estimates in Ontario, Canada, Hydrology and Earth System Sciences, 24, 4887–4902, https://doi.org/10.5194/hess-24-4887-2020, 2020.

Kouki, K., Luojus, K., and Riihelä, A.: Evaluation of snow cover properties in ERA5 and ERA5-Land with several satellite-based datasets in the Northern Hemisphere in spring 1982–2018, The Cryosphere, 17, 5007–5026, https://doi.org/10.5194/tc-17-5007-2023, 2023.

Laprise, R., de Elía, R., Caya, D., Biner, S., Lucas-Picher, P., Diaconescu, E., Leduc, M., Alexandru, A., Separovic, L., and Canadian Network for Regional Climate Modelling and Diagnostics: Challenging some tenets of regional climate modelling, Meteorol. Atmos. Phys., 100, 3–22, https://doi.org/10.1007/s00703-008-0292-9, 2008.

Lievens, H., Demuzere, M., Marshall, H.-P., Reichle, R. H., Brucker, L., Brangers, I., De Rosnay, P., Dumont, M., Girotto, M., Immerzeel, W. W., Jonas, T., Kim, E. J., Koch, I., Marty, C., Saloranta, T., Schöber, J., and De Lannoy, G. J. M.: Snow depth variability in the Northern Hemisphere mountains observed from space, Nat Commun, 10, https://doi.org/10.1038/s41467-019-12566-y, 2019.

Lindsay, R., Wensnahan, M., Schweiger, A., and Zhang, J.: Evaluation of Seven Different Atmospheric Reanalysis Products in the Arctic, Journal of Climate, 27, 2588–2606, https://doi.org/10.1175/JCLI-D-13-00014.1, 2014.

Loprieno, Raffa, Campanale, and Mercogliano: VHR-REA_IT: Transitioning from COSMO-CLM to ICON-CLM at convection-permitting scales, Fondazione CMCC Centro Euro-Mediterraneo sui Cambiamenti Climatici, Lecce, Italy, 2024.

Main-Knorn, M., Pflug, B., Louis, J., Debaecker, V., Müller-Wilm, U., and Gascon, F.: Sen2Cor for Sentinel-2, in: Image and Signal Processing for Remote Sensing XXIII, Image and Signal Processing for Remote Sensing XXIII, 37–48, https://doi.org/10.1117/12.2278218, 2017.

Majidi, F., Sabetghadam, S., Gharaylou, M., and Rezaian, R.: Evaluation of the performance of ERA5, ERA5-Land and MERRA-2 reanalysis to estimate snow depth over a mountainous semi-arid region in Iran, Journal of Hydrology: Regional Studies, 58, 102246, https://doi.org/10.1016/j.ejrh.2025.102246, 2025.

Masson, V., Le Moigne, P., Martin, E., Faroux, S., Alias, A., Alkama, R., Belamari, S., Barbu, A., Boone, A., Bouyssel, F., Brousseau, P., Brun, E., Calvet, J.-C., Carrer, D., Decharme, B., Delire, C., Donier, S., Essaouini, K., Gibelin, A.-L., Giordani, H., Habets, F., Jidane, M., Kerdraon, G., Kourzeneva, E., Lafaysse, M., Lafont, S., Lebeaupin Brossier, C., Lemonsu, A., Mahfouf, J.-F., Marguinaud, P., Mokhtari, M., Morin, S., Pigeon, G., Salgado, R., Seity, Y., Taillefer, F., Tanguy, G., Tulet, P., Vincendon, B., Vionnet, V., and Voldoire, A.: The SURFEXv7.2 land and ocean surface platform for coupled or offline simulation of earth surface variables and fluxes, Geosci. Model Dev., 6, 929–960, https://doi.org/10.5194/gmd-6-929-2013, 2013.

Matiu, M. and Hanzer, F.: Bias adjustment and downscaling of snow cover fraction projections from regional climate models using remote sensing for the European Alps, Hydrology and Earth System Sciences, 26, 3037–3054, https://doi.org/10.5194/hess-26-3037-2022, 2022.

https://doi.org/10.5194/egusphere-2026-2484
Preprint. Discussion started: 20 May 2026

Matiu, M., Crespi, A., Bertoldi, G., Carmagnola, C. M., Marty, C., Morin, S., Schöner, W., Cat Berro, D., Chiogna, G., De Gregorio, L., Kotlarski, S., Majone, B., Resch, G., Terzago, S., Valt, M., Beozzo, W., Cianfarra, P., Gouttevin, I., Marcolini, G., Notarnicola, C., Petitta, M., Scherrer, S. C., Strasser, U., Winkler, M., Zebisch, M., Cicogna, A., Cremonini, R., Debernardi, A., Faletto, M., Gaddo, M., Giovannini, L., Mercalli, L., Soubeyroux, J.-M., Sušnik, A., Trenti, A., Urbani, S., and Weilguni, V.: Observed snow depth trends in the European Alps: 1971 to 2019, The Cryosphere, 15, 1343–1382, https://doi.org/10.5194/tc-15-1343-2021, 2021.

Mätzler, C.: Applications of the interaction of microwaves with the natural snow cover, Remote Sensing Reviews, 2, 259–387, https://doi.org/10.1080/02757258709532086, 1987.

Miglietta, M. M. and Davolio, S.: Dynamical forcings in heavy precipitation events over Italy: lessons from the HyMeX SOP1 campaign, Hydrology and Earth System Sciences, 26, 627–646, https://doi.org/10.5194/hess-26-627-2022, 2022.

Mirza, B. N., Small, E. E., and Raleigh, M. S.: Evaluating the utility of Sentinel-1 in a Data Assimilation System for estimating snow depth in a mountainous basin, The Cryosphere, 19, 6691–6709, https://doi.org/10.5194/tc-19-6691-2025, 2025.

Moccia, B., Buonora, L., Bertini, C., Ridolfi, E., Russo, F., and Napolitano, F.: What is our pick? Assessment of satellite and reanalysis precipitation datasets over Italy, Journal of Hydrology: Regional Studies, 60, 102487, https://doi.org/10.1016/j.ejrh.2025.102487, 2025.

Montanari, A., Nguyen, H., Rubinetti, S., Ceola, S., Galelli, S., Rubino, A., and Zanchettin, D.: Why the 2022 Po River drought is the worst in the past two centuries, Science Advances, 9, eadg8304, https://doi.org/10.1126/sciadv.adg8304, 2023.

Monteiro, D. and Morin, S.: Multi-decadal analysis of past winter temperature, precipitation and snow cover data in the European Alps from reanalyses, climate models and observational datasets, The Cryosphere, 17, 3617–3660, https://doi.org/10.5194/tc-17-3617-2023, 2023.

Mott, R., Winstral, A., Cluzet, B., Helbig, N., Magnusson, J., Mazzotti, G., Quéno, L., Schirmer, M., Webster, C., and Jonas, T.: Operational snow-hydrological modeling for Switzerland, Front. Earth Sci., 11, https://doi.org/10.3389/feart.2023.1228158, 2023.

Mudryk, L., Mortimer, C., Derksen, C., Elias Chereque, A., and Kushner, P.: Benchmarking of snow water equivalent (SWE) products based on outcomes of the SnowPEx+ Intercomparison Project, The Cryosphere, 19, 201–218, https://doi.org/10.5194/tc-19-201-2025, 2025.

Muñoz-Sabater, J., Dutra, E., Agustí-Panareda, A., Albergel, C., Arduini, G., Balsamo, G., Boussetta, S., Choulga, M., Harrigan, S., Hersbach, H., Martens, B., Miralles, D. G., Piles, M., Rodríguez-Fernández, N. J., Zsoter, E., Buontempo, C., and Thépaut, J.-N.: ERA5-Land: a state-of-the-art global reanalysis dataset for land applications, Earth System Science Data, 13, 4349–4383, https://doi.org/10.5194/essd-13-4349-2021, 2021.

National Operational Hydrologic Remote Sensing Center: Snow Data Assimilation System (SNODAS) Data Products at NSIDC, Version 1, National Snow and Ice Data Center (NSIDC), Boulder, Colorado, USA, https://doi.org/10.7265/N5TB14TC, last access: 22.04.2026, 2004.

Pfeffer, W. T., Arendt, A. A., Bliss, A., Bolch, T., Cogley, J. G., Gardner, A. S., Hagen, J.-O., Hock, R., Kaser, G., Kienholz, C., Miles, E. S., Moholdt, G., Mölg, N., Paul, F., Radić, V., Rastner, P., Raup, B. H., Rich, J., Sharp, M. J., and The Randolph Consortium: The Randolph Glacier Inventory: a globally complete inventory of glaciers, J. Glaciol., 60, 537–552, https://doi.org/10.3189/2014JoG13J176, 2014.

Pflug, J. M., Kumar, S. V., Livneh, B., Gutmann, E. D., Gangrade, S., and Kao, S. C.: Comparisons of montane snow water equivalent projections: calculating total snow mass in regions with projection agreement and divergence in the western United States, J. Climate, 38, 855–874, https://doi.org/10.1175/JCLI-D-24-0073.1, 2025.

Pimentel, R., Herrero, J., and Polo, M. J.: Subgrid parameterization of snow distribution at a Mediterranean site using terrestrial photography, Hydrol. Earth Syst. Sci., 21, 805–820, https://doi.org/10.5194/hess-21-805-2017, 2017.

Raffa, M., Reder, A., Marras, G. F., Mancini, M., Scipione, G., Santini, M., and Mercogliano, P.: VHR-REA_IT Dataset: Very High Resolution Dynamical Downscaling of ERA5 Reanalysis over Italy by COSMO-CLM, Data, 6, 88, https://doi.org/10.3390/data6080088, 2021.

https://doi.org/10.5194/egusphere-2026-2484
Preprint. Discussion started: 20 May 2026

Rajulapati, C. R., Papalexiou, S. M., Clark, M. P., Razavi, S., Tang, G., and Pomeroy, J. W.: Assessment of Extremes in Global Precipitation Products: How Reliable Are They?, Journal of Hydrometeorology, 21, 2855–2873, https://doi.org/10.1175/JHM-D-20-0040.1, 2020.

Raleigh, M. S., Lundquist, J. D., and Clark, M. P.: Exploring the impact of forcing error characteristics on physically based snow simulations within a global sensitivity analysis framework, Hydrology and Earth System Sciences, 19, 3153–3179, https://doi.org/10.5194/hess-19-3153-2015, 2015.

Ridal, M., Bazile, E., Le Moigne, P., Randriamampianina, R., Schimanke, S., Andrae, U., Berggren, L., Brousseau, P., Dahlgren, P., Edvinsson, L., El-Said, A., Glinton, M., Hagelin, S., Hopsch, S., Isaksson, L., Medeiros, P., Olsson, E., Unden, P., and Wang, Z. Q.: CERRA, the Copernicus European Regional Reanalysis system, Quarterly Journal of the Royal Meteorological Society, 150, 3385–3411, https://doi.org/10.1002/qj.4764, 2024.

Rockel, B., Will, A., and Hense, A.: The Regional Climate Model COSMO-CLM (CCLM), metz, 17, 347–348, https://doi.org/10.1127/0941-2948/2008/0309, 2008.

Sabetghadam, S., Fletcher, C. G., and Erler, A.: The importance of model horizontal resolution for improved estimation of snow water equivalent in a mountainous region of western Canada, Hydrology and Earth System Sciences, 29, 887–902, https://doi.org/10.5194/hess-29-887-2025, 2025.

Santanello, J. A., Dirmeyer, P. A., Ferguson, C. R., Findell, K. L., Tawfik, A. B., Berg, A., Ek, M., Gentine, P., Guillod, B. P., Heerwaarden, C. van, Roundy, J., and Wulfmeyer, V.: Land–Atmosphere Interactions: The LoCo Perspective, Bulletin of the American Meteorological Society, 99, 1253–1272, https://doi.org/10.1175/BAMS-D-17-0001.1, 2018.

Sarigil, G., Neri, M., and Toth, E.: Evaluation of national and international gridded meteorological products for rainfall-runoff modelling in Northern Italy, Journal of Hydrology: Regional Studies, 56, 102031, https://doi.org/10.1016/j.ejrh.2024.102031, 2024.

Schrodin, R. and Heise, E.: The Multi-Layer Version of the DWD Soil Model TERRA_LM, COSMO Technical Report No. 2, Deutscher Wetterdienst, Offenbach, Germany, 16 pp., https://doi.org/10.5676/DWD_pub/nwv/cosmo-tr_2, 2001.

Soci, C., Bazile, E., Besson, F., and Landelius, T.: High-resolution precipitation re-analysis system for climatological purposes, Tellus A: Dynamic Meteorology and Oceanography, 68, 29879, https://doi.org/10.3402/tellusa.v68.29879, 2016.

Soci, C., Hersbach, H., Simmons, A., Poli, P., Bell, B., Berrisford, P., Horányi, A., Muñoz-Sabater, J., Nicolas, J., Radu, R., Schepers, D., Villaume, S., Haimberger, L., Woollen, J., Buontempo, C., and Thépaut, J.-N.: The ERA5 global reanalysis from 1940 to 2022, Quarterly Journal of the Royal Meteorological Society, 150, 4014–4048, https://doi.org/10.1002/qj.4803, 2024.

Sourp, L., Pedinotti, V., Alonso-González, E., Jarlan, L., and Gascoin, S.: Assessment of Snow Cover Fraction Parameterizations for High Resolution Snowpack Reanalyses, Hydrological Processes, 40, 4, e70491, https://doi.org/10.1002/hyp.70491, 2026.

Takala, M., Luojus, K., Pulliainen, J., Derksen, C., Lemmetyinen, J., Kärnä, J.-P., Koskinen, J., and Bojkov, B.: Estimating northern hemisphere snow water equivalent for climate research through assimilation of space-borne radiometer data and ground-based measurements, Remote Sensing of Environment, 115, 3517–3529, https://doi.org/10.1016/j.rse.2011.08.014, 2011.

Terzago, S., Andreoli, V., Arduini, G., Balsamo, G., Campo, L., Cassardo, C., Cremonese, E., Dolia, D., Gabellani, S., von Hardenberg, J., Morra di Cella, U., Palazzi, E., Piazzi, G., Pogliotti, P., and Provenzale, A.: Sensitivity of snow models to the accuracy of meteorological forcings in mountain environments, Hydrology and Earth System Sciences, 24, 4061–4090, https://doi.org/10.5194/hess-24-4061-2020, 2020.

Urraca, R. and Gobron, N.: Temporal stability of long-term satellite and reanalysis products to monitor snow cover trends, The Cryosphere, 17, 1023–1052, https://doi.org/10.5194/tc-17-1023-2023, 2023.

Verrelle, A., Michael, G., Eric, B., and Moigne, P. L.: Strengths and weaknesses of the new CERRA-Land surface reanalysis at 5.5 km resolution over Europe, Copernicus Meetings, https://doi.org/10.5194/ems2022-279, 2022.

Vionnet, V., Brun, E., Morin, S., Boone, A., Faroux, S., Le Moigne, P., Martin, E., and Willemet, J.-M.: The detailed snowpack scheme Crocus and its implementation in SURFEX v7.2, Geosci. Model Dev., 5, 773–791, https://doi.org/10.5194/gmd-5-773-2012, 2012.

https://doi.org/10.5194/egusphere-2026-2484
Preprint. Discussion started: 20 May 2026

Viviroli, D., Dürr, H., Messerli, B., Meybeck, M., and Weingartner, R.: Mountains of the world, water towers for humanity: Typology, mapping, and global significance, Water Resources Research, 43, https://doi.org/10.1029/2006WR005653, 2007.